ASTRONOMY & ASTROPHYSICS
SUPPLEMENT SERIES

Astron. Astrophys. Suppl. Ser. **115,** 439-468 (1996)

A CO survey of galaxies with the SEST and the 20-m Onsala telescope*

T. Elfhag[1], R.S. Booth[2], B. Höglund[2], L.E.B. Johansson[2] and Aa. Sandqvist[1]

[1] Stockholm Observatory, S-133 36 Saltsjöbaden, Sweden
[2] Onsala Space Observatory, S-439 92 Onsala, Sweden

Received May 2; accepted September 4, 1995

Abstract. — A large survey of galaxies in the J=1−0 CO line, performed during 1985-1988 using the 15-m SEST and the 20-m millimetre wave telescope of Onsala Space Observatory, is presented. The HPBW of the telescopes are 44″ and 33″ at 115 GHz, respectively. The central positions of 168 galaxies were observed and 101 of these were detected in the CO line. More than 20% of these are new detections. Maps of some of the galaxies are also presented.

Key words: galaxies: ISM — radio lines: ISM

1. Introduction

The study of carbon monoxide (CO) in space began in our own Galaxy with the observations of the Orion Nebula by Wilson et al. (1970). Rickard et al. (1975) made the first detection of extragalactic CO by observing M 82 and NGC 253. The long timespan between the detection of Galactic and extragalactic CO was entirely due to lack of receiver sensitivity. Not until 1974-75 did millimetre wavelength receivers become sensitive enough to detect nearby galaxies strong in CO. Today, with good SIS receivers it is possible to detect substantially weaker emission and thereby improve our knowledge regarding gas content in all kinds of galaxies.

A number of extragalactic CO surveys, performed with different telescopes, are now present in the literature (Verter 1990). Some examples are Stark et al. (1987) using the Bell Labs 7-m telescope, Solomon & Sage (1988), Sage (1993) and Young et al. (1995) using the NRAO 12-m and the FCRAO 14-m telescopes, Mirabel et al. (1990) using the 15-m SEST and Braine et al. (1993) using the IRAM 30-m telescope. Observation of CO is one of few means we have to measure the potential for star formation in external galaxies. With sufficient resolution it can directly give us the locations and approximate sizes of the star forming regions. CO intensities also seem to correlate well with other star formation indicators such as infrared and radio continuum radiation (Braine & Combes 1992).

In this paper we present a survey of 168 galaxies observed in the J=1−0 CO line with the 15-m SEST and the Onsala Space Observatory (OSO) 20-m millimetre wave telescope. This sample of galaxies is not complete, the merit of the survey lies in its size. The galaxies were primarily chosen from the samples of Balzano (1983), Hummel (1980), Keel (1983) and Stauffer (1982). The 40 southern galaxies, observed with the SEST, were chosen from the IRAS catalogue, with the criteria $S(60\ \mu\mathrm{m}) > 8$ Jy and negative declinations ($\delta < 0°$). Of the 168 galaxies observed, 101 were detected in CO, i.e. 60%. More than 20% of these are new detections, not previously published. The rest of the sample has also been observed with other telescopes having different diameters and we briefly compare with a few of these results.

2. Observations and data reduction

The observations in the ^{12}CO $J = 1-0$ line were performed during 1985-1987 using the OSO 20-m radome-enclosed millimetre wave telescope and in 1988 using the 15-m SEST.

Approximately the first half of the OSO observations were performed with a Schottky barrier diode mixer and the latter half with a SIS mixer. The single-sideband system temperatures at the feed horn ranged from 300 to 500 K (Schottky) and from 150 to 300 K (SIS), depending on receiver status, weather and elevation. Pointing of the telescope was checked before each observing run using planets, NGC 7027 and IRC +10216, and was found to be accurate within 5″. The beamwidth and main beam efficiency of the telescope at 115 GHz were 33″ and 0.3

Send offprint requests to: Aa. Sandqvist
*Tables 1 and 2 are also available in electronic form at CDS via ftp 130.79.128.5

Table 1. Properties of galaxies detected in the J=1−0 CO Line

Galaxy	Right ascension (1950) h m s	Declination (1950) o ' "	$\int T_{mb}\,dV$ {K km s^{-1}}	V_{LSR} {km s^{-1}}	(V_{HEL} −V_{LSR}) {km s^{-1}}	Previous Detections	Type	Optical Diameter (') (mb's) (Tel)	log L_{CO} {K km s^{-1} pc^2}	log L_{IR} {$L_\odot$}	log L_B {$L_\odot$}
(1)	(2)	(3)	(4)	(5)	(6)	(7)	(8)	(9)	(10)	(11)	(12)
NGC 23	00 07 18.6	25 38 48	18.0 ±1.3	4535	−4	0,1,2,5,20	SB(s)a	2.1 3.8 O	9.51	11.27	11.23
NGC 134	00 27 53.6	−33 31 09	22.5 ±1.2	1545	7	new	SAB(s)bc	8.5 11.6 S	8.89	10.78	11.09
NGC 157	00 32 13.8	−08 40 23	16.5 ±1.1	1675	4	0,3,4,19	SAB(rs)bc	4.2 5.7 S	8.85	10.80	11.03
NGC 174	00 34 31.5	−29 45 09	9.5 ±0.7	3515	7	new	SB(rs)0/a:	1.4 1.9 S	9.21	11.07	10.50
NGC 278	00 49 14.7	47 16 46	10.9 ±0.9	650	−5	0,3	SAB(rs)b	2.1 3.8 O	7.77	10.33	10.35
NGC 337	00 57 19.9	−07 50 52	2.7 ±0.7	1725	5	0	SB(s)d	2.9 4.0 S	8.05	10.42	10.68
NGC 613	01 31 59.1	−29 40 32	34.4 ±1.1	1465	11	new	SB(rs)bc	5.5 7.5 S	9.01	10.75	10.90
NGC 660	01 40 20.7	13 23 32	58.3 ±4.6	880	5	0,1,3,6,8,24	SB(s)a pec	8.3 15.1 O	8.62	10.75	10.16
NGC 772	01 56 35.2	18 45 57	13.8 ±1.8	2335	5	0,1	SA(s)b	7.2 13.1 O	8.86	10.88	11.39
NGC 864	02 12 49.8	05 46 10	3.5 ±1.1	1500	8	0,2,3	SAB(rs)c	4.7 6.4 S	8.11	9.97	10.70
NGC 908	02 20 46.7	−21 27 35	12.2 ±0.8	1380	13	0	SA(s)c	6.0 8.2 S	8.57	10.69	10.98
NGC 986	02 31 34.3	−39 15 48	36.2 ±0.7	1945	14	6	SB(rs)ab	3.9 5.3 S	9.27	10.91	10.77
NGC 992	02 34 35.6	20 53 04	15.6 ±4.2	4055	6	5,8	S?	0.9 1.6 O	9.35	11.22	10.85
NGC 1022	02 36 04.7	−06 53 30	5.7 ±0.8	1425	12	0,13	(R')SB(s)	2.4 3.3 S	8.26	10.57	10.36
NGC 1055	02 39 11.2	00 13 44	28.0 ±3.0	995	11	0,1,3	SBb: sp	7.6 13.8 O	8.36	10.45	10.51
NGC 1084	02 43 32.3	−07 47 12	14.5 ±0.7	1375	12	0,1,3	SA(s)c	3.2 4.4 S	8.60	10.73	10.72
NGC 1187	03 00 23.7	−23 03 43	7.0 ±0.7	1300	15	new	SB(r)c	5.5 7.5 S	8.24	10.32	10.61
NGC 1326	03 22 01.7	−36 38 23	7.5 ±1.0	1355	17	12,16	(R)SB(r)0+	3.9 5.3 S	8.22	10.01	10.48
NGC 1365	03 31 41.8	−36 18 27	106.0 ±1.7	1610	17	11,28	SB(s)b	11.2 15.3 S	9.56	11.20	11.20
NGC 1385	03 35 19.7	−24 39 48	5.6 ±0.9	1470	17	0	SB(s)cd	3.4 4.6 S	8.20	10.50	10.63
NGC 1406	03 37 21.7	−31 29 03	9.0 ±1.1	1060	17	new	SB(s)bc:sp	3.8 5.2 S	8.07	9.98	10.18
UGC 2855	03 43 09.5	69 58 46	28.0 ±3.1	1135	−5	1	SABc	4.4 8.0 O	8.62	10.93	10.59
NGC 1482	03 52 25.8	−20 38 54	33.6 ±1.6	1830	17	0,5	SA0+ pec	2.5 3.4 S	9.13	10.83	10.03
NGC 1511	03 59 24.5	−67 46 32	6.4 ±0.7	1255	15	new	SAa pec	3.5 4.8 S	8.10	10.41	10.41
NGC 1530	04 17 03.0	75 10 42	24.0 ±2.4	2435	−6	0,1,2	SB(rs)b	4.6 8.4 O	9.12	10.90	11.06
NGC 1614	04 31 35.8	−08 40 57	15.2 ±1.1	4700	17	0,2,5,6	SB(s)c pec	1.3 1.8 S	9.68	11.77	10.82
NGC 2146	06 10 40.1	78 22 23	88.6 ±2.8	885	−6	0,1,2,3,6,13,15	SB(s)ab pec	6.0 10.9 O	8.88	11.20	10.59
NGC 2268	07 00 47.6	84 27 41	18.3 ±3.3	2320	−8	new	SAB(r)bc	3.2 5.8 O	8.92	10.56	10.89
NGC 2276	07 10 31.3	85 50 51	15.8 ±1.0	2400	13	0,1,2,4,6	SAB(rs)c	2.8 5.1 O	8.93	10.98	10.91
NGC 2339	07 05 25.6	18 51 34	25.8 ±4.0	2230	−9	0,1,2	SAB(rs)bc	2.7 4.9 O	8.97	10.86	10.86
NGC 2369	07 16 03.9	−62 15 07	35.1 ±1.1	3185	16	10	SB(s)a	3.5 4.8 S	9.67	11.22	10.99
NGC 2403	07 32 03.0	65 42 24	10.8 ±3.5	165	−3	0,2	SAB(s)cd	21.9 39.8 O	6.65	8.74	10.13
NGC 2559	08 15 02.4	−27 18 13	32.6 ±1.1	1525	17	0	SB(s)bc pec:	3.7 5.0 S	8.93	10.65	11.35
NGC 2633	08 42 34.2	74 17 00	18.5 ±3.0	2185	−6	0,1,2,4	SB(s)b	2.5 4.5 O	8.89	10.91	10.60
NGC 2681	08 49.58.0	51 30 12	7.7 ±1.7	685	5	0,3,14	(R')SAB(rs)0/a:	3.6 6.5 O	7.51	9.55	10.16
NGC 2683	08 49 34.8	33 36 31	20.2 ±2.9	415	0	0,9	SA(rs)b	9.3 16.9 O	7.35	9.19	10.08
NGC 2782	09 10 53.6	40 19 15	9.1 ±2.0	2545	2	0,1,4,7,8	SAB(rs)a pec	3.5 6.4 O	8.68	10.72	10.80
NGC 2798	09 14 08.4	42 12 42	8.1 ±1.9	1700	2	0,1,2,4	SB(s)a pec	2.6 4.7 O	8.29	10.74	10.28
NGC 2964	09 39 57.0	32 04 30	30.7 ±4.1	1325	3	0,1,3,4	SAB(r)bc:	2.9 5.3 O	8.61	10.25	10.37
NGC 3079	09 58 35.2	55 55 13	93.5 ±6.3	1145	−3	0,1,2,3,4,6,17	SB(s)c	7.9 14.4 O	9.02	10.79	10.77
IC 2554	10 07 30.2	−66 47 08	10.6 ±1.2	1345	12	new	SB(s)bc pec:	3.1 4.2 S	8.29	10.20	11.03
NGC 3175	10 12 24.6	−28 37 24	19.3 ±1.4	1085	12	new	SAB(s)a?	5.0 6.8 S	8.33	9.92	10.19
NGC 3294	10 33 24.1	37 35 05	5.2 ±3.0	1550	−1	new	SA(s)c	3.5 6.4 S	8.27	10.31	10.65
NGC 3344	10 40 46.6	25 11 10	9.1 ±3.4	600	1	0,2,3,7	(R)SAB(r)bc	7.1 12.9 O	7.31	9.47	10.04
NGC 3351	10 41 19.1	11 57 58	25.0 ±3.1	750	4	0,3,9,15,18	SB(r)b	7.4 13.4 O	7.96	9.87	10.35
NGC 3471	10 56 02.2	61 47 56	14.9 ±4.8	2115	−6	20	Sa	1.7 3.1 O	8.77	10.57	10.33
NGC 3521	11 03 15.1	00 13 58	26.8 ±4.8	725	4	0,2	SAB(rs)bc	11.0 20.0 O	7.99	10.35	10.73
NGC 3556	11 08 36.8	55 56 33	16.0 ±2.1	705	−6	0,1,2	SB(s)cd sp	8.7 5.8 O	7.87	10.38	10.63
NGC 3593	11 11 59.7	13 05 22	28.7 ±5.3	605	1	0,9,12	SA(s)0/a:	5.2 9.4 O	7.83	9.64	9.68
NGC 3620	11 14 23.5	−75 56 33	47.0 ±1.6	1775	11	new	(R')SB(s)ab pec	2.8 3.8 S	9.33	11.09	
NGC 3631	11 18 12.9	53 26 39	12.1 ±1.7	1160	−6	0,7	SA(s)c	5.0 9.1 O	8.16	10.28	10.58
NGC 3810	11 38 24.5	11 44 51	19.5 ±2.7	975	−0	0,1,3,7	SAB(rs)c	4.3 7.8 O	8.12	10.08	10.33
NGC 4041	11 59 38.7	62 24 59	21.2 ±3.0	1245	−9	0,1	SA(rs)bc:	2.7 4.9 O	8.48	10.49	10.34
NGC 4088	12 03 00.9	50 49 12	23.1 ±2.5	765	−8	0	SAB(rs)bc	5.8 10.5 O	8.10	10.34	10.42
NGC 4102	12 03 50.8	52 59 21	36.4 ±5.5	830	−8	0,8	SAB(s)b?	3.0 5.5 O	8.39	10.62	10.07
NGC 4157	12 08 33.4	50 45 44	19.9 ±3.1	735	−8	0,1	SAB(s)b? sp	6.8 12.4 O	8.06	10.29	10.25
NGC 4194	12 11 41.7	54 48 21	12.0 ±1.8	2525	−9	0,1,5,13	IBm pec	1.8 3.3 O	8.81	11.15	10.47
NGC 4217	12 13 21.2	47 22 17	12.8 ±3.3	1055	−8	new	Sb sp	5.2 9.5 O	8.08		10.33
NGC 4414	12 23 57.1	31 29 56	29.2 ±5.0	710	−7	0,1,3,9	SA(rs)c?	3.6 6.5 O	8.09	10.26	10.33
NGC 4418	12 24 20.3	−00 36 09	4.5 ±0.9	2105	−2	0,5	(R')SAB(s)a	1.4 1.9 S	8.44	11.17	10.27
NGC 4536	12 31 53.9	02 27 42	20.2 ±2.6	1790	−3	0,1,2,8	SAB(rs)bc	7.6 13.8 O	8.68	10.84	11.03

Table 1. continued

NGC 4565	12 33 51.8	26 15 50	14.8 ±2.5	1295	−7	3,25,27	SA(s)b? sp	15.8	28.7	O	8.25	10.32	11.33
NGC 4568	12 34 03.0	11 30 45	35.5 ±3.4	2230	−4	0,1,2,21	SA(rs)bc	4.6	8.4	O	9.14	11.08	11.01
NGC 4579	12 35 12.6	12 05 40	23.1 ±5.0	1460	−5	0,1,2,3,21	SAB(rs)b	5.9	10.7	O	8.60	10.30	11.01
NGC 4691	12 45 39.5	−03 03 28	7.3 ±0.9	1125	−3	0,16,23	(R)SB(s)0/apec	2.8	3.8	S	8.03	10.05	10.18
NGC 5033	13 11 08.0	36 51 48	31.3 ±4.9	995	−10	0,1,3,6,7,11	Sa(s)c	10.7	19.5	O	8.33	10.24	10.64
NGC 5055	13 13 35.4	42 17 48	41.1 ±1.5	515	−11	0,6,9	SA(rs)bc	12.6	22.9	O	8.03	10.43	10.69
IC 883	13 18 18.3	34 23 53	4.1 ±1.2	6745	−10	2,5	Im:pec	1.5	2.7	O	9.20	11.80	10.76
NGC 5218	13 30 27.4	63 01 24	24.8 ±2.9	2900	−12	6	SB(s)b?pec	1.8	3.3	O	9.23	10.80	10.59
NGC 5371	13 53 34.2	40 42 23	6.5 ±2.1	2685	−13	new	SAB(rs)bc	4.4	8.0	O	8.56	10.73	11.17
NGC 5430	13 59 08.3	59 34 10	25.3 ±6.2	2970	−13	5	SB(s)b	2.2	4.0	O	9.31	11.05	10.87
NGC 5660	14 28 00.1	49 50 58	10.0 ±3.1	2315	−14	new	SAB(rs)c	2.8	5.1	O	8.68	10.42	10.73
NGC 5676	14 31 01.4	49 40 37	20.7 ±4.1	2115	−14	0,4	SA(rs)bc	4.0	7.3	O	8.92	10.87	10.97
NGC 5678	14 30 37.1	58 08 35	18.3 ±2.9	1785	−14	0,4	SAB(rs)b	3.3	6.0	O	8.80	10.77	10.75
II ZW 71	14 49 13.1	35 44 53	9.8 ±2.6	1545	−15	new	Pec	1.0	1.8	O	8.16		9.36
NGC 5907	15 14 34.8	56 30 33	12.5 ±3.3	630	−15	0,3,26	SA(s)c: sp	12.6	22.9	O	7.83	10.27	10.74
NGC 6000	15 46 44.1	−29 14 08	20.4 ±1.3	2160	−8	0	SB(s)bc:	1.9	2.6	S	9.09	11.10	10.54
NGC 6156	16 30 28.2	−60 30 55	16.0 ±0.7	3245	−18	new	SAB(rs)c pec:	1.6	2.2	S	9.35	11.16	11.72
NGC 6181	16 30 09.4	19 55 48	10.6 ±2.2	2350	1	0,4	SAB(rs)c	2.5	4.5	O	8.72	10.82	10.88
NGC 6217	16 35 02.8	78 17 58	16.9 ±2.2	1365	−13	0,1,3,4	(R)SB(rs)bc	3.0	5.5	O	8.51	10.48	10.51
IC 4687	18 09 20.2	−57 44 28	8.2 ±0.9	5130	−1	10	Sb: pec	1.3	1.8	S	9.48	11.55	10.74
NGC 6574	18 09 34.8	14 58 00	23.4 ±3.4	2330	−19	0,2	SAB(rs)bc?	1.4	2.5	O	9.05	10.93	10.85
NGC 6643	18 21 14.0	74 32 42	30.0 ±5.8	1520	−14	0,1,2,4,7	SA(rs)c	3.8	6.9	O	8.84	10.65	10.79
IC 4734	18 34 08.4	−57 32 05	13.1 ±0.8	4600	−1	10	(R')SB(s)abpec:	1.3	1.8	S	9.60	11.44	
NGC 6764	19 07 01.2	50 51 08	9.3 ±2.1	2425	−18	8	SB(s)bc	2.3	4.2	O	8.72	10.65	10.78
NGC 6792	19 19 22.1	43 02 15	6.2 ±2.5	4570	−19	new	SBb	2.2	4.0	O	9.07	10.56	11.33
NGC 6810	19 39 20.9	−58 46 30	17.4 ±1.5	1945	0	new	SA(s)ab:sp	3.2	5.8	O	8.70	10.76	10.75
NGC 6835	19 51 45.9	−12 42 00	9.1 ±0.9	1585	−13	new	SB(s)a?sp	2.3	3.1	S	8.59	10.50	10.45
NGC 6907	20 22 08.0	−24 58 20	21.2 ±1.1	3150	−9	4	SB(s)bc	3.3	4.5	S	9.50	11.17	11.25
NGC 6951	20 36 36.6	65 55 54	23.3 ±4.6	1740	−15	0,18,19	SAB(rs)bc	3.9	7.1	O	8.70	10.62	10.94
NGC 7130	21 45 19.7	−35 11 04	14.3 ±0.5	4820	−2	6	Sa pec	1.5	2.0	S	9.68	11.52	11.01
IC 5179	22 13 12.9	−37 05 39	14.9 ±1.0	3400	−0	10	SA(rs)bc	2.3	3.1	S	9.40	11.33	11.09
NGC 7331	22 34 47.7	34 09 35	26.9 ±3.7	755	−11	0,2,3	SA(s)b	10.5	19.1	O	8.36	10.80	11.07
NGC 7448	22 57 34.8	15 42 50	14.1 ±3.2	2230	−7	0,4	SA(rs)bc	2.7	4.9	O	8.80	10.69	10.94
NGC 7469	23 00 44.4	08 36 19	16.9 ±2.5	4860	−6	0,1,2,5,11,22	(R')SAB(rs)a	1.5	2.7	O	9.54	11.76	11.14
NGC 7479	23 02 26.4	12 03 06	32.8 ±4.1	2375	−6	0,1,2,4	SB(s)c	4.1	7.5	O	9.23	10.97	11.12
NGC 7496	23 06 59.4	−43 41 54	4.0 ±0.6	1630	4	new	SB(s)b	3.3	4.5	S	8.18	10.30	10.48
NGC 7541	23 12 12.1	04 15 46	67.3 ±8.6	2705	−4	0,1,2,4	SB(rs)bc: pec	3.5	6.4	O	9.63	11.22	11.07
NGC 7603	23 16 22.6	−00 01 39	17.1 ±4.7	8785	−3	new	SA(rs)b: pec	1.5	2.7	O	10.04	10.89	11.26
NGC 7625	23 17 59.4	16 57 12	20.6 ±4.3	1605	−6	0,1,2,12	SA(rs)a pec	1.6	2.9	O	8.73	10.49	10.23
NGC 7771	23 48 52.1	19 49 57	31.2 ±2.1	4235	−4	0,1,5	SB(s)a	2.5	4.5	O	9.70	11.60	11.09

References [Telescope diameter]: 0 - Young et al. (1995) [14 m]; 1 - Solomon & Sage (1988) [14, 12 m]; 2 - Young et al. (1989) [14 m]; 3 - Braine et al. (1993) [30 m]; 4 - Tinney et al. (1990) [12 m]; 5 - Sanders et al. (1991) [12 m]; 6 - Aalto et al. (1991)[20, 15 m]; 7 - Stark et al. (1987) [7 m]; 8 - Sanders & Mirabel (1985) [12, 14 m]; 9 - Sage (1993) [12 m]; 10 - Mirabel et al. (1990) [15 m]; 11 - Heckman et al. (1989) [12 m]; 12 - Wiklind & Henkel (1989) [30, 20, 15 m]; 13 - Devereux et al. (1994) [45 m]; 14 - Taniguchi et al. (1994) [45 m]; 15 - Jackson et al. (1989) [14 m]; 16 - Tacconi et al. (1991) [15 m]; 17 - Schöniger & Sofue (1994) [45 m]; 18 - Kenney et al. (1992) [OVRO interferometer]; 19 - Elmegreen & Elmegreen (1982) [11 m]; 20 - Chini et al. (1992) [15, 30 m]; 21 - Stark et al. (1986) [7 m]; 22 - Taniguchi et al. (1990) [45 m]; 23 - Wiklind et al. (1993) [30 m]; 24 - van Driel et al. (1995) [45m]; 25 - Richmond & Knapp (1986) [7 m]; 26 - Sofue (1994) [45 m]; 27 - Sofue & Nakai (1994) [45 m]; 28 - Sandqvist et al. (1988) [12 m].

respectively (Elldér, private communication). The spectra were obtained with a 512×1 MHz filter bank, yielding a velocity resolution of 2.6 km s^{-1}. Velocity is given with respect to the local standard of rest (LSR). A dual-beam switch mode, with a beam separation of about 12′, was used, placing the source alternately in the two beams to eliminate asymmetry. Only linear baselines have been removed and the resultant spectra have been "boxcar" smoothed to four times their original resolution in velocity, namely 10.4 km s^{-1}.

During June 1988 additional observations were done of a few low declination objects (NGC 864, NGC 4418, NGC 4536 and NGC 4691) and one southern object (NGC 1365) with the 15-m Swedish ESO Submillimetre Telescope (SEST) at La Silla, Chile. The southern IRAS galaxies were observed in October and December 1988. SEST was equipped with a Schottky barrier diode mixer and was used together with a 728-channel acousto-optical spectrometer, which yielded a velocity resolution of 1.8 km s^{-1}. The system temperatures, corrected to above the atmosphere, were in the range 300−500 K and the beamwidth of the telescope was 44″. Main beam efficiency at 115 GHz was 0.66 in June and 0.73 in October and December (after re-alignment of the reflector surface), forward spillover and scattering efficiency equal to 0.92. Pointing accuracy was measured to be about 3″ rms. As

Table 2. Galaxies searched for CO, with negative results

Galaxy	Right ascension (1950) h m s	Declination (1950) o ' "	Velocity* (km s^{-1})	RMS (T_{mb}) {K}	Type
NGC 232	00 40 17.5	-23 50 02	1500+	0.04	SB(r)a? pec
NGC 262	00 46 04.9	31 41 04	4490	0.04	SA(s)0/a
NGC 315	00 55 05.8	30 04 58	4920	0.04	E+:
IC 1623	01 05 18.1	-17 46 36	1500+	0.04	-
NGC 449	01 13 19.6	32 49 32	4880	0.04	(R')S?
NGC 925	02 24 16.7	33 21 22	560	0.05	Sa
NGC 1052	02 38 37.0	-08 28 05	1500	0.02	E4
NGC 1084	02 43 31.8	-07 47 08	1400	0.05	SA(s)c
NGC 1222	03 06 24.1	-03 08 48	2710	0.04	S0 pec
NGC 1266	03 13 28.5	-02 36 43	1500	0.04	(R')SB(rs)0°pec
E420-G13	04 11 53.2	-32 07 59	1500	0.04	SA(r)0+pec
NGC 1637	04 38 57.5	-02 57 11	715	0.05	SAB(rs)c
NGC 1964	05 31 14.1	-21 58 46	480	0.04	SAB(s)c
NGC 2110	05 49 46.4	-07 28 03	2285	0.05	SAB0
MCG 811011	05 51 09.6	46 25 51	6150	0.03	SB?
Ma 3	06 09 49.0	71 03 10	3950	0.03	S0:
NGC 2347	07 11 16.1	64 48 01	4420	0.04	SB(r)ab? pec
NGC 2377	07 22 33.0	-09 33 36	2400	0.03	SA(s)c:
Ma 79	07 38 47.2	49 55 50	6645	0.03	SBb
NGC 2523	08 09 15.5	73 43 50	3450	0.04	SA(s)b:?
NGC 2639	08 40 03.0	50 23 14	3315	0.03	(R)SA(r)a:?
NGC 2655	08 49 08.3	78 24 48	1390	0.04	SAB(s)0/a
NGC 2942	09 36 07.7	34 13 51	4500	0.02	SA(s)c:
NGC 3183	10 17 33.0	74 25 38	2000	0.03	SB(s)bc:
NGC 3303	10 34 17.9	18 23 48	6400	0.03	pec
NGC 3359	10 43 20.7	63 29 12	1120	0.04	SB(rs)c
NGC 3412	10 48 14.9	13 40 27	860	0.04	SB(s)0
NGC 3432	10 49 42.5	36 53 07	620	0.03	SB(s)m sp
E93 - 3	10 57 29.3	-66 03 16	1470	0.04	SAB(r)0/a?
NGC 3486	10 57 41.9	29 14 36	680	0.03	SAB(r)c
NGC 3489	10 57 40.6	14 10 13	600	0.10	SAB0+
NGC 3516	11 03 22.8	72 50 24	2600	0.04	RSB(s)0°:
NGC 3735	11 33 03.2	70 48 42	2700	0.04	SAc: sp
NGC 3813	11 38 40.2	36 49 29	1450	0.04	SA(rs)b:
NGC 3998	11 55 19.9	55 40 03	1100	0.03	SA(r)0?
NGC 4111	12 04 31.6	43 20 41	820	0.04	SA(r)0+sp
NGC 4151	12 08 00.0	39 40 52	995	0.03	(R')SAB(rs)ab:
NGC 4260	12 16 48.8	06 22 40	1850	0.02	SB(s)a
NGC 4261	12 16 50.3	06 06 06	2180	0.04	E2+
NGC 4374	12 22 31.4	13 09 49	910	0.04	E1
NGC 4382	12 22 53.2	18 28 03	770	0.04	SA(s)0+pec
NGC 4500	12 29 02.6	58 14 26	3000	0.04	SB(s)a
NGC 4559	12 33 29.4	28 14 07	810	0.04	SAB(rs)cd
Ma 231	12 54 05.0	57 08 39	12300	0.03	SA(rs)c? pec
NGC 5297	13 44 18.9	44 07 22	2600	0.04	SAB(s)c: sp
NGC 5322	13 47 35.1	60 26 21	1800	0.04	E3+
NGC 5363	13 53 36.6	05 29 58	1140	0.02	I0?
NGC 5364	13 53 41.2	05 15 37	1500	0.04	SA(rs)bc pec
NGC 5394	13 56 25.2	37 41 39	3500	0.03	SB(s)b pec
NGC 5395	13 56 29.7	37 40 02	3500	0.04	SA(s)b pec
NGC 5548	14 15 43.7	25 21 59	5175	0.03	(R')SA(s)0/a
NGC 5675	14 30 36.6	36 31 18	4290	0.04	S?
NGC 5850	15 04 35.5	01 44 17	2500	0.04	SB(r)b
NGC 5860	15 04 44.3	42 49 53	5400	0.03	S?
NGC 6251	16 37 58.5	82 38 19	6900	0.04	E
NGC 6384	17 29 58.6	07 05 46	1800	0.02	SAB(r)bc
IC 4662	17 42 13.5	-64 37 16	310	0.04	IBm
NGC 6500	17 53 48.1	18 20 40	2980	0.04	SAab
NGC 6824	19 42 36.6	55 59 23	3300	0.04	SA(s)b:
NGC 6918	20 27 15.4	-47 38 33	1500++	0.04	(R')SB(r)0/a:
NGC 7217	22 05 37.9	31 06 53	900	0.04	(R)SA(r)ab
NGC 7241	22 13 27.3	18 59 01	1450	0.03	SB(s)bc? pec
NGC 7316	22 33 30.6	20 03 50	5550	0.03	S
NGC 7332	22 35 01.2	23 32 16	1200	0.06	S0 pec sp
NGC 7468	23 00 30.2	16 20 08	2090	0.04	E3: pec
NGC 7674	23 25 24.4	08 30 06	8660	0.03	SA(r)bc pec
NGC 7714	23 33 40.6	01 52 41	2805	0.04	SB(s)b: pec

*
+ a search was also carried out at a velocity of 2500 km s^{-1}
++ searches were also carried out at velocities of 2500, 3500 and 4500 km s^{-1}

with the OSO data only first order polynomials have been subtracted and the spectra have been boxcar smoothed to a resolution of 7.4 km s^{-1} for the June data and 10.3 km s^{-1} for the October and December data.

The observed intensities, T_A^*, are chopper-wheel calibrated and are related to the main beam brightness temperature, T_{mb}, which is appropriate for a source filling the main beam, by $T_A^* = T_{mb} \times$ (main beam efficiency). The OSO data were checked for consistency by repeated observations of NGC 7027 and IRC +10216 using the values T_{mb}=5.2 K and T_{mb}=11.5 K, respectively (Olofsson 1983).

3. Results

3.1. *CO survey*

CO was detected in 101 galaxies and the results are presented in Table 1 and Fig. 1. Table 1 identifies the galaxies in Col. (1) and gives the central positions in Cols. (2) and (3). The integrated CO line intensities, $I_{CO} = \int T_{mb}\, dV$, are given in Col. (4) and the CO centroid velocities with respect to the local standard of rest are given in Col. (5). To correct to the heliocentric (HEL) frame of reference we have included the appropriate difference ($V_{HEL} - V_{LSR}$) in Col. (6). References to previous detections, as obtained from a search in the SIMBAD database, are listed in Col. (7) where "new" implies no previous observations published in refereed journals. Galaxy types according to de Vaucouleurs et al. (1991) (RC3) are listed in Col. (8). Column (9) gives the optical diameters, D_{25} in arcmin, as presented in RC3. In addition, these optical diameters are given relative to the main beam size (mb's) of the telescope which is identified by the notation "O" for the Onsala 20-m telescope and "S" for the 15-m SEST. Column (10) gives the calculated CO luminosities, $L_{CO} = I_{CO}\pi d^2/4$, where d(pc) is the linear half-power diameter of the telescope main beam, using the radial velocity with respect to the Galactic Standard of Rest obtained from RC3 and assuming $H_0 = 50$ km s^{-1} Mpc^{-1}. In Col. (11) we present infrared luminosities obtained in a manner similar to Young et al. (1989) [$L_{IR} = 3.75\ 10^5\ D^2 C(2.58\ S_{60} + S_{100})$]. Finally, the Blue light luminosities (L_B) - calculated using values of B_T^0 obtained from RC3, $M_{Bo} = 5.48$ and $H_0 = 50$ km s^{-1} Mpc^{-1} - are given in Col. (12).

We have calculated errors in the CO integrated line intensities and these are also listed in Col. (4). These errors are dependent on the inherent rms noise fluctuations of the profiles and the uncertainties in subtracting baselines. The line uncertainty, assuming a perfect baseline, is given by

$$\Delta I_{line} = \frac{\sigma}{\sqrt{n}} \cdot \Delta\nu = \sigma\sqrt{\frac{B}{N} \cdot \Delta\nu} \qquad (1)$$

where N is the total number of spectrometer channels covering a total velocity range of B km s^{-1}, $\Delta\nu$ km s^{-1} is the total velocity width of the spectral line, n is the

number of channels covered by the spectral line and σ is the rms noise per channel. Assuming only linear baselines, which is the case for all our observations, the baseline fitting uncertainty is given by

$$\Delta I_{\rm base} = \sigma \cdot \Delta\nu \sqrt{\frac{B}{N}\frac{1}{B-\Delta\nu}} \quad (2)$$

and the total error in the integrated line intensity is

$$\Delta I = \sqrt{\Delta I_{\rm line}^2 + \Delta I_{\rm base}^2} = \frac{\sigma}{\sqrt{N}} \cdot B \sqrt{\frac{\Delta\nu}{B-\Delta\nu}} \quad (3)$$

An examination of the optical diameters in Col. (9) indicates that many of the galaxies are resolved by our observations, implying that the calculated $L_{\rm CO}$ represents a lower limit to the total CO luminosity for a specific galaxy. In some cases, however, such as the very distant galaxies and/or those with a high degree of central CO concentration, the tabulated value approaches the total CO luminosity. This is further discussed in Sect. 3.2.

The spectra of CO emission, observed in the central positions of the detected galaxies, are presented in Fig. 1. The galaxies have been ordered according to increasing right ascension.

Thirty of the 101 detected galaxies have a central $L_{\rm CO}$ larger than or equal to 10^9 K km s^{-1} pc^2. They form an interesting subgroup, which might deserve special attention. Due to their large amount of gas they may be potential starburst galaxies. Two more galaxies (NGC 660 and NGC 2146 - see also Fig. 5 in Sect. 4) have values of $L_{\rm CO}$ less than 10^9 K km s^{-1} pc^2 but still deserve special attention due to their high values of $I_{\rm CO}$. We briefly present these galaxies below.

NGC 23 is a barred spiral galaxy in pair with NGC 26. The gas velocity field in its central region has been studied by Afanas'ev et al. (1991) using the 6-m optical telescope in the Caucasus. They suggest that NGC 23 may be in a post-Seyfert stage.

NGC 174 is a barred spiral galaxy with a ring-like structure.

NGC 613 is a barred spiral galaxy with an active hot spot nucleus, a radio jet and a circumnuclear radio ring; there is some evidence for an accelerated collimated outflow (Hummel et al. 1987).

NGC 660 is discussed by Braine et al. (1993). It is a peculiar galaxy with a prominent central bar-like structure and a strongly warped outer disk structure. H I and OH has been observed in absorption towards the nucleus by Baan et al. (1992) using the VLA. van Driel et al. (1995) have recently presented a thorough study of this galaxy in the optical and radio spectral regions.

NGC 986 is a barred spiral which has been observed both in the ^{12}CO and ^{13}CO $J = 1-0$ lines by Aalto et al. (1991).

NGC 992 is a spiral galaxy possibly interacting with Mrk 369. It has been observed in the radio continuum by Condon et al. (1982) using the VLA.

NGC 1365 has the highest $I_{\rm CO}$ value of all our observed galaxies, namely 106.0 K km s^{-1}. It is a barred spiral Seyfert 1.5 galaxy in the Fornax cluster with a circumnuclear ring of starburst activity signposts. It has been mapped extensively in the radio continuum with the VLA and in the $J = 2-1$ and $1-0$ CO emission lines with the SEST by Sandqvist et al. (1982, 1995), and with the NRAO Kitt Peak 12-m millimetre wave telescope by Sandqvist et al. (1988). The H I distribution and velocity field has been mapped with the VLA by Jörsäter & van Moorsel (1995). NGC 1365 does not have any companion.

NGC 1482 is a peculiar IR-luminous galaxy with detected molecular hydrogen in the nucleus, as observed in the near-infrared lines by Kawara et al. (1987).

NGC 1530 is a Sersic-Pastoriza galaxy which has been mapped with the VLA in the 20-cm continuum by Saikia et al. (1994) and with the 91-m telescope in the 21-cm H I line by Rots (1981). The HCN $J = 1-0$ line (as well as the CO $J = 1-0$ line) has been observed with the 30-m telescope by Solomon et al. (1992).

NGC 1614 is an IR-luminous merger with barred structure which has been observed extensively in the optical, infrared and radio regions by Neff et al. (1990). Interferometric observations of CO have been performed by Scoville et al. (1989).

NGC 2146 is discussed by Braine et al. (1993). It is a peculiar SB galaxy with a complex optical morphology and enhanced star-forming activity. It has recently been observed at a number of positions in the ^{12}CO and ^{13}CO $J = 2-1$ and $1-0$ as well as the CS $J = 2-1$ lines by Xie et al. (1994) using the 14-m FCRAO telescope.

NGC 2369 is a barred spiral galaxy.

NGC 3079 is discussed by Braine et al. (1993). It is a peculiar nearly edge-on SB galaxy with a violent bipolar outflow of gas from the nucleus, a "galactic superwind" (Filippenko & Sargent 1992). H I in absorption against the nucleus has been detected by Gallimore et al. (1994) using the VLA. NGC 3079 has also been observed in the CO $J = 1-0$ line by Sofue & Irwin (1992) using the Nobeyama mm array.

NGC 3620 is a peculiar southern SB galaxy with a prominent differential velocity across the nucleus, seen in optical emission lines (Schwartz 1978). The two optical velocity components, 2.″5 east and west of the nucleus, have heliocentric velocities of 1638±9 and 1919±33 km s^{-1}, respectively, which are very close to the values of the two major peaks in the CO profile (see Fig. 1).

NGC 4568 is a Virgo cluster spiral galaxy in contact with NGC 4567. High-resolution optical CCD spectra (Rubin et al. 1989) and VLA H I observations (Guhathakurta et al. 1988) have revealed its optical and radio rotation curves.

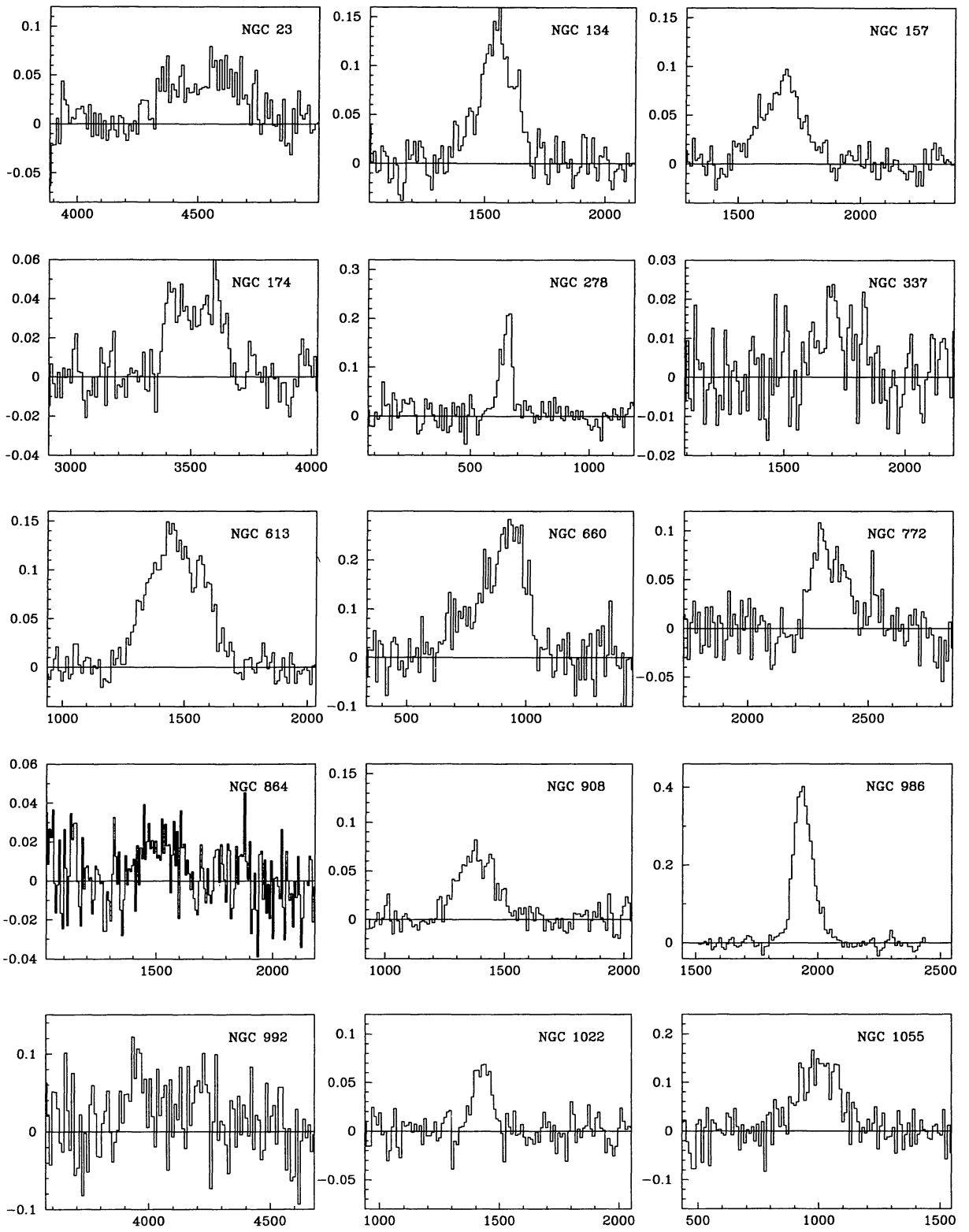

Fig. 1. $J = 1{-}0$ CO emission line profiles observed at the central positions of the galaxies listed in Table 1. The ordinate is the main beam brightness temperature, $T_{\rm mb}$ (K) and the abcissa is the radial velocity (km s^{-1}) with respect to the local standard of rest. The velocity resolution is 10.3 or 10.4 km s^{-1}, with the exception of NGC 864, NGC 1365, NGC 4418, NGC 4536 and NGC 4691 which all have a velocity resolution of 7.4 km s^{-1}

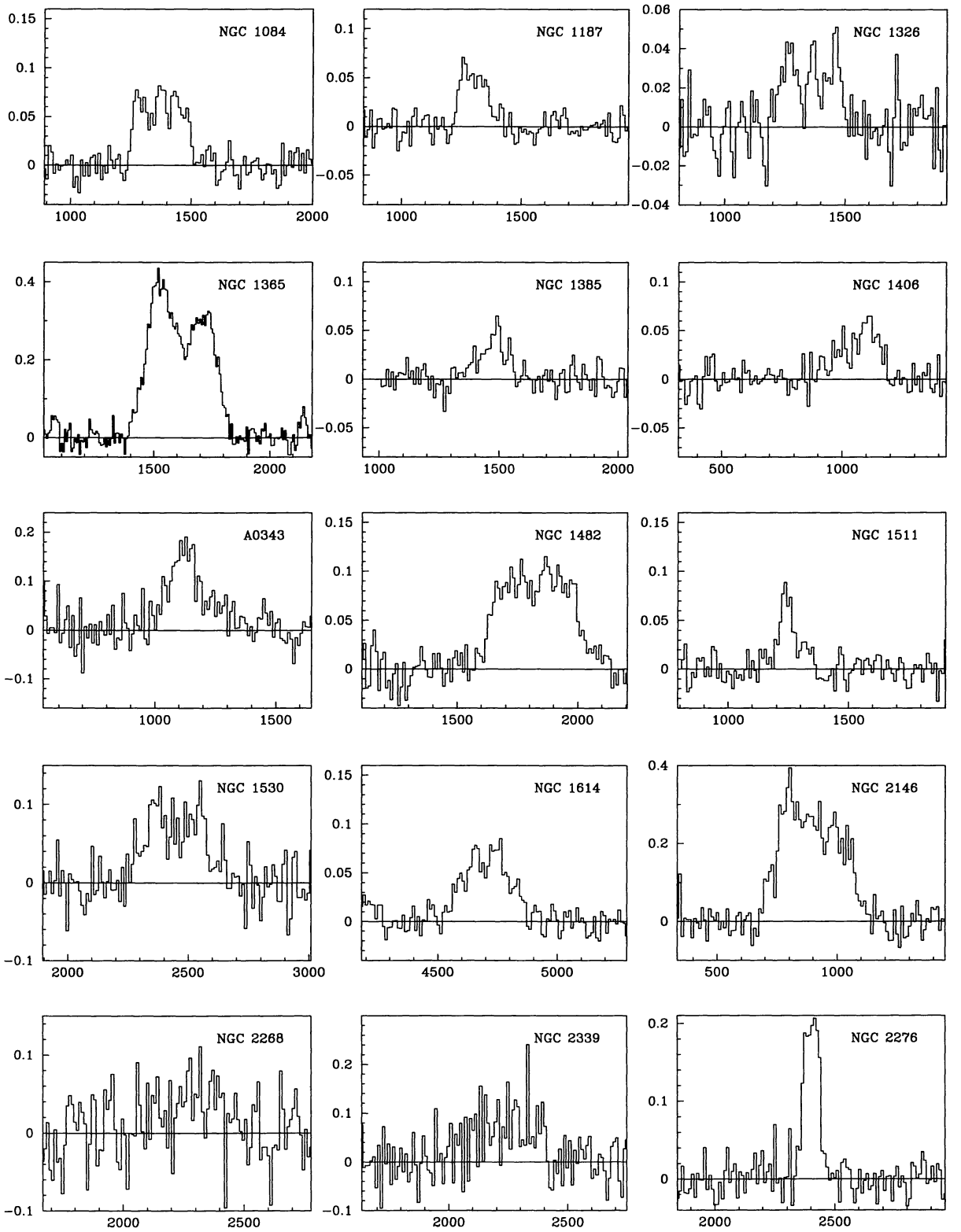

Fig. 1. continued

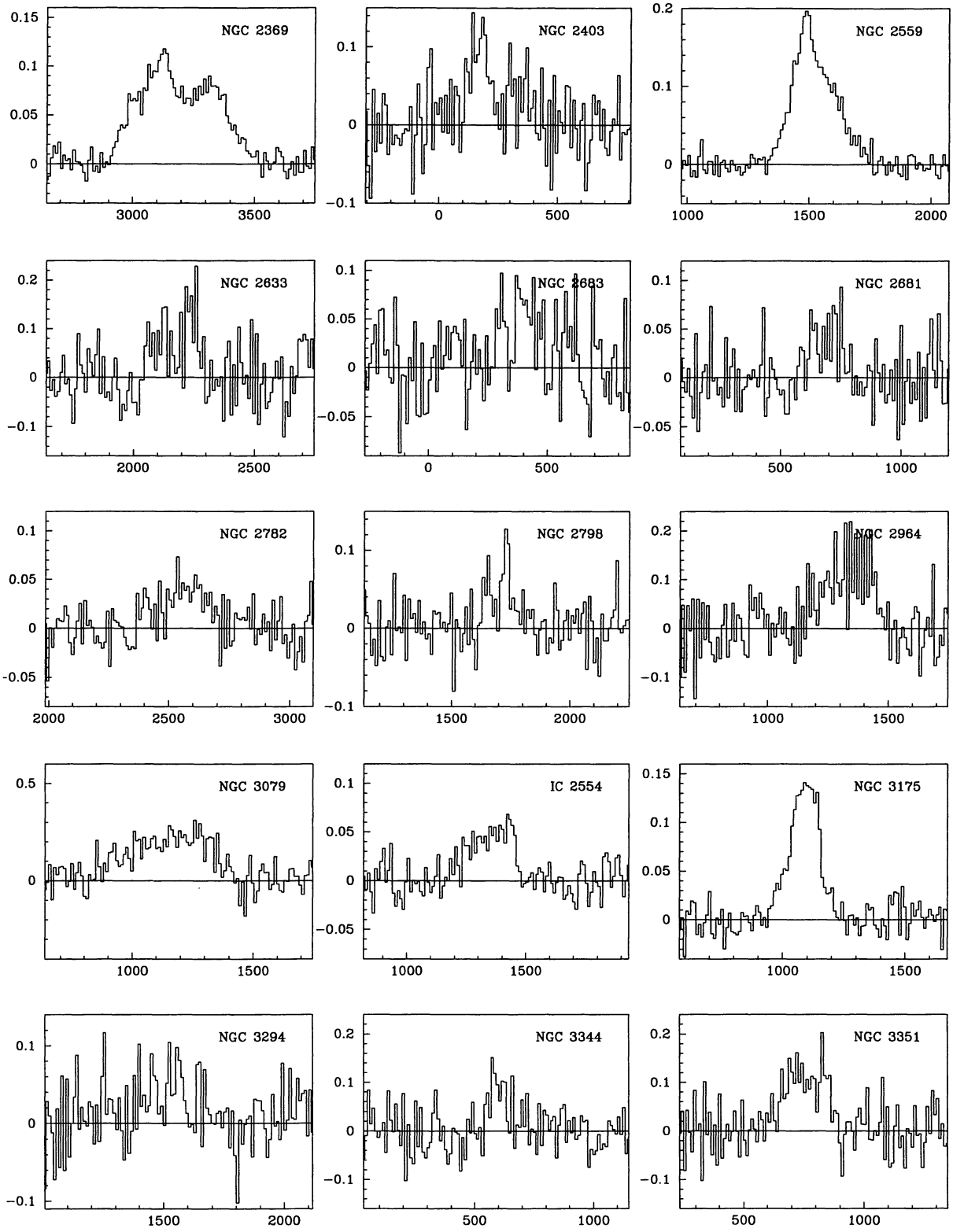

Fig. 1. continued

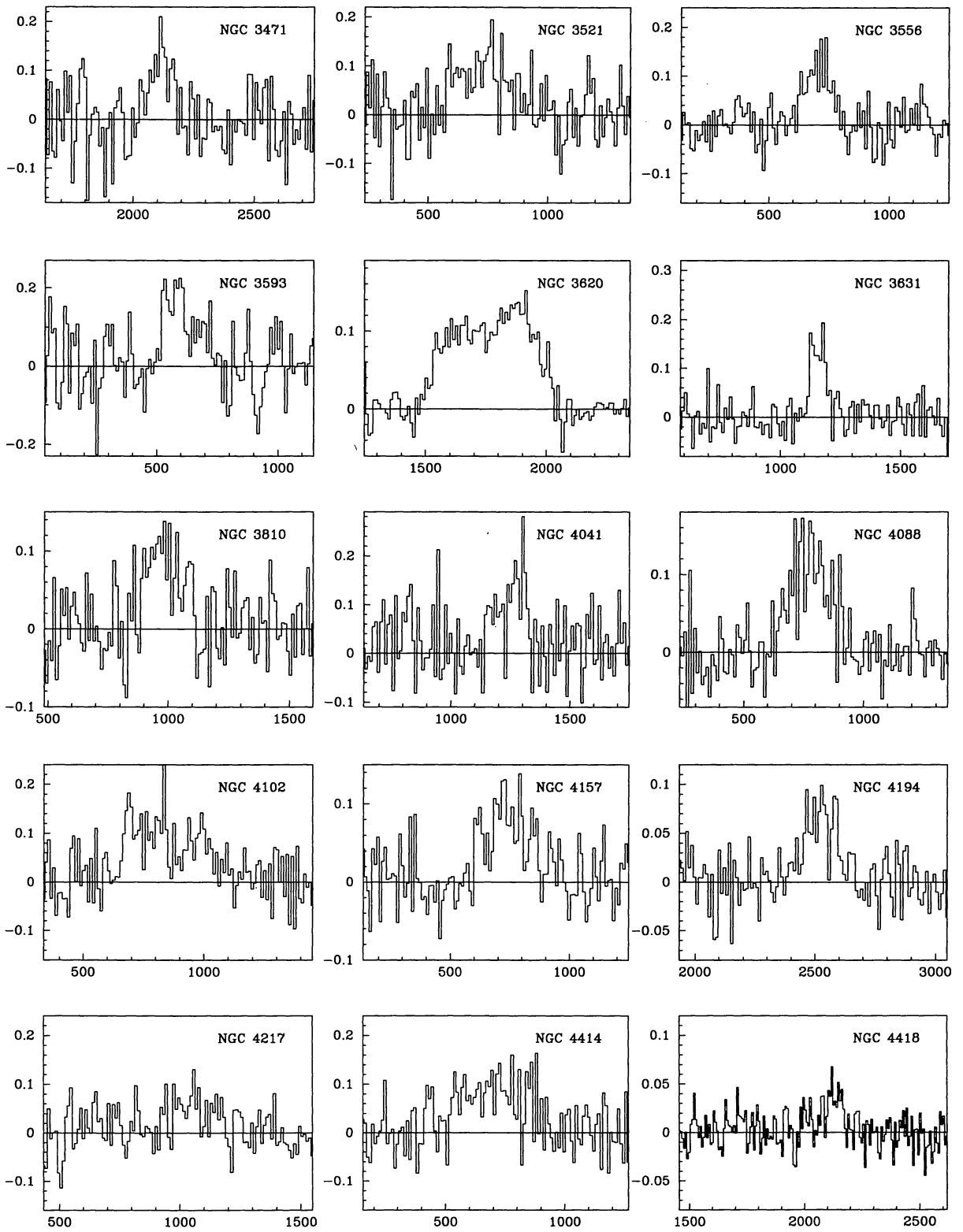

Fig. 1. continued

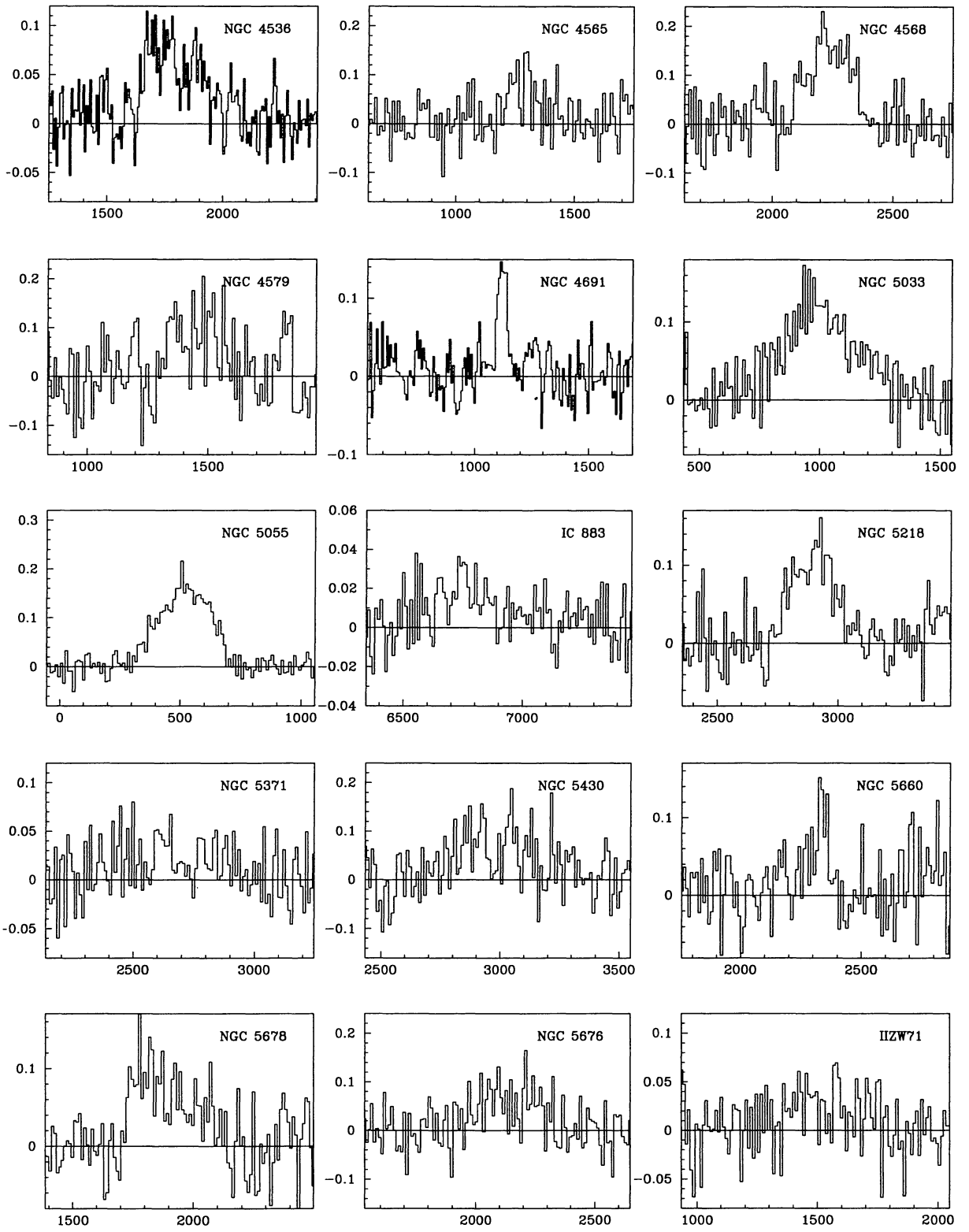

Fig. 1. continued

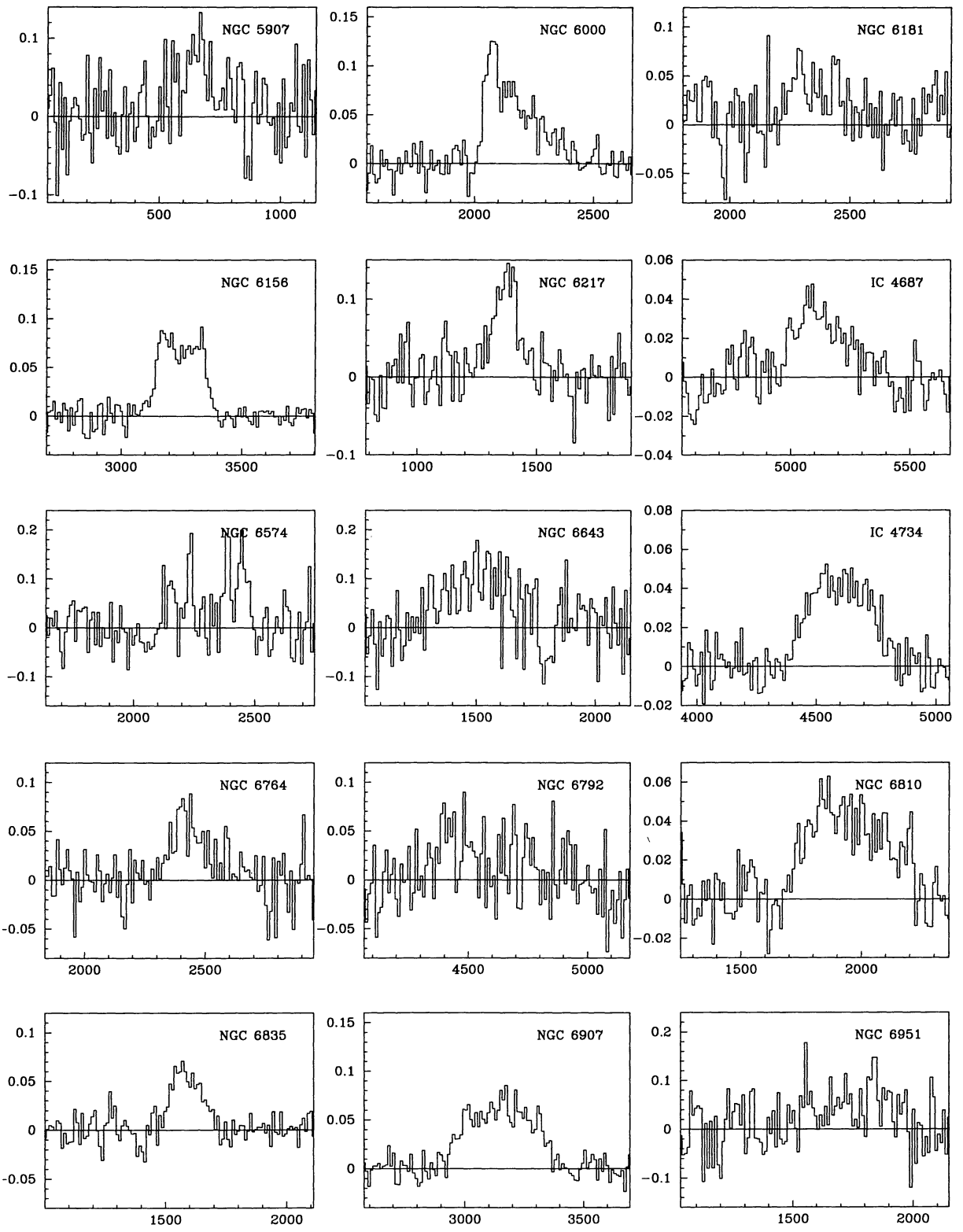

Fig. 1. continued

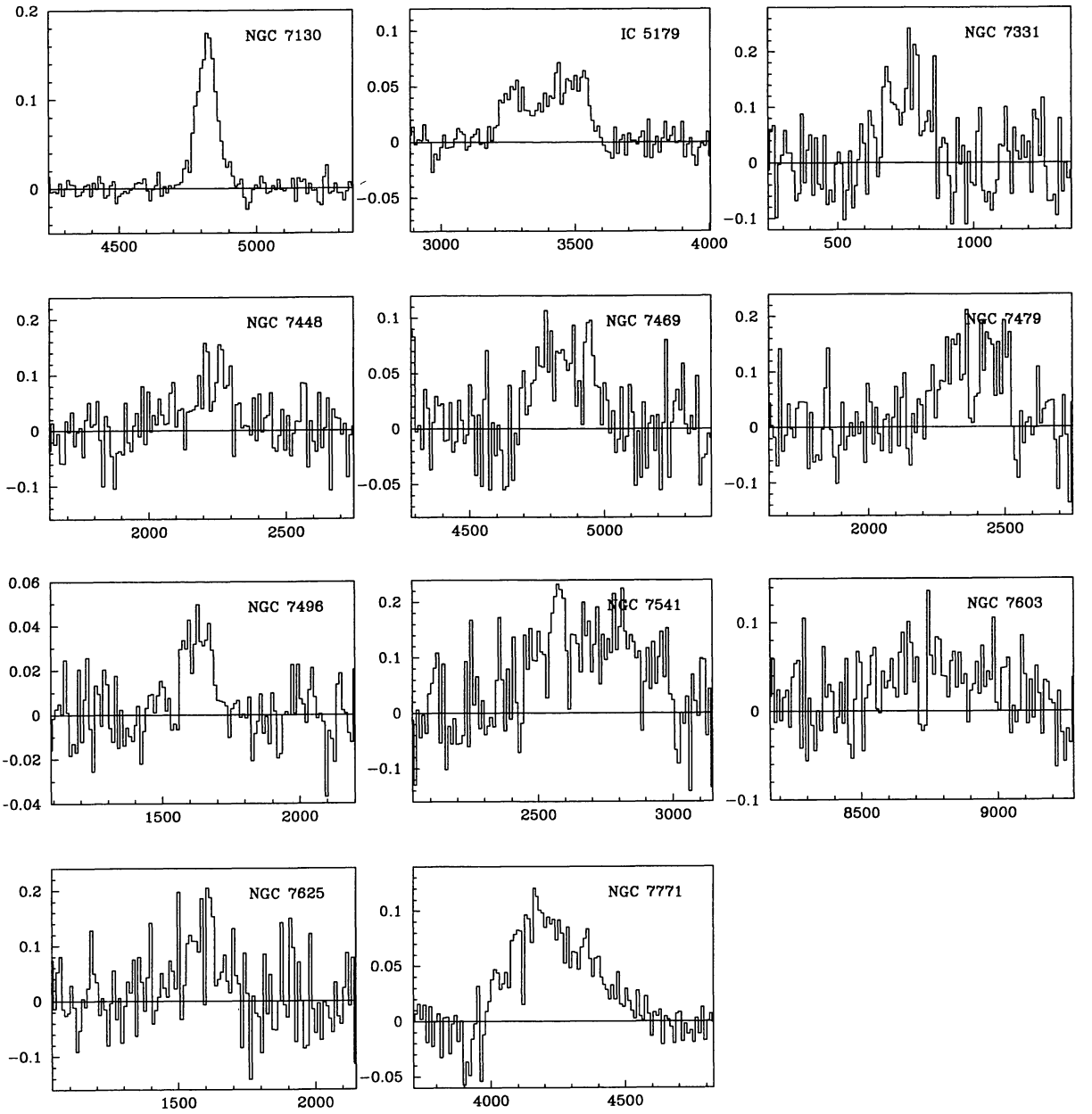

Fig. 1. continued

IC 883, also known as Arp 193, is an example of an advanced disk-disk merger of interacting galaxies. It has been imaged in the near-infrared JHK bands by Stanford & Bushouse (1991).

NGC 5218 is a barred spiral galaxy, interacting with NGC 5216, which has been observed both in the ^{12}CO and ^{13}CO $J = 1-0$ lines by Aalto et al. (1991).

NGC 5430 is a barred spiral galaxy containing an extremely luminous H II region showing very strong Wolf-Rayet emission features (Keel 1987). It has been observed in the radio continuum by Condon et al. (1982) using the VLA.

NGC 6000 is a typical starburst galaxy (SB) with bright nuclear H II regions. It has been observed in the submillimetre and millimetre continuum regions by Roche & Chandler (1993) using the 15-m JCMT on Mauna Kea. There is no evidence for any excess emission above the cool dust emission.

NGC 6156 is a peculiar barred spiral galaxy.

IC 4687 is a peculiar spiral galaxy interacting with IC 4686 and IC 4689. All three galaxies show enhanced infrared activity (Lutz 1992).

NGC 6574 has been mapped in the mm-continuum by Chini et al. (1995) with the SEST and in the 6-cm continuum by Condon et al. (1991) with the VLA.

IC 4734 is a peculiar luminous infrared galaxy, with barred structure.

NGC 6792 is a barred spiral galaxy in the Hercules region on which accurate CCD surface photometry in the I-band has been performed by Freudling et al. (1991) and which has been observed in the 21-cm H I line by Tifft & Cocke (1988) using the 91-m radio telescope.

NGC 6907 is a barred spiral galaxy, which has been observed in the 6- and 20-cm radio continuum with the VLA (Beck 1991).

NGC 7130 is a peculiar spiral galaxy.

IC 5179 is a luminous infrared galaxy.

NGC 7469 is a Seyfert 1 SAB galaxy in pair with IC 5283. It has a partial circumnuclear radio and optical ring showing starburst activity (Wilson et al. 1991). It has been observed with ROSAT (Brandt et al. 1993).

NGC 7479 is a SBc non-interacting galaxy which seems to maintain a leading density wave that triggers star formation by developing a shock front (Beckman & Cepa 1990). Schöniger & Sofue (1994) present CO and H I observations.

NGC 7541 is a peculiar galaxy in pair with NGC 7537. Its optical rotation curve has been determined by Rubin et al. (1978) and Kyazimov (1980). It has been observed in the radio continuum by van der Hulst et al. (1981) using the VLA.

NGC 7603 is a Seyfert galaxy which has shown variability from type Seyfert 1 to Seyfert 1.9 and back again to Seyfert 1 over a period of about a decade (Goodrich 1989). It has been observed in the radio continuum by van der Hulst et al. (1981) using the VLA.

NGC 7771 is a SBa galaxy which together with NGC 7770 makes an interacting pair of galaxies. It has a strong UV excess. Detailed surface photometry has been carried out in the blue spectral band by Osman (1986).

Nine of these 32 galaxies show indications of physical interaction with another galaxy, 25 are barred spirals or show bar-like structure. Of these 25, five belong to the former group and five are peculiar. That 75% of the high-CO-luminosity galaxies are barred may indicate that a signifcant fraction of our CO detections are barred galaxies. More significant, however, may be that of the 67 galaxies in which no CO was detected (see Table 2) 60% do not show barred structures. In the case of the barred spirals, gas dynamics transports the gas inwards along the bars, leading to concentration of large amount of gas in the central regions of these galaxies and thus creating prerequisite conditions for rapid starburst activity.

A few of the detections shown in Fig. 1 are rather weak, e.g. NGC 2268, NGC 2683, NGC 3294, NGC 4217, NGC 4565, NGC 5371, NGC 6574, NGC 6792, NGC 6951 and NGC 7603. To examine the reality of the CO detections, we investigated the H I velocities and profile widths for these galaxies using the General Catalog of H I Observations of Galaxies (Huchtmeier & Richter 1989). For most cases the H I and CO velocities agree within a few tens of km s^{-1} (the H I profile widths are generally of the order of 400 km s^{-1}). For NGC 6951, $V_{\rm HI}$ is about 1415 km s^{-1} and $V_{\rm CO}$ about 1740 km s^{-1}, a difference of more than 300 km s^{-1}. However, Elmegreen & Elmegreen (1982a) report detection of weak CO emission at 1525 and 1669 km s^{-1} in NGC 6951 and Kenney et al. (1992) have mapped the CO emission with the OVRO interferometer, although they present no velocity information. We therefore believe in the reality of our CO detections.

Table 2 presents the galaxies in which no CO was detected at the central positions. The velocity (with respect to the local standard of rest) is the velocity of the central channel of the spectrometer during the search. The RMS value is defined by the noise deviations ($T_{\rm mb}$ units) at a velocity resolution of 10 km s^{-1}.

3.2. *CO luminosities*

In Fig. 2 we present plots of the central CO luminosities of our survey galaxies, listed in Table 1, as a function of the IR ($L_{\rm IR}$) and blue ($L_{\rm B}$) luminosities. We present also the relationship with the total radio continuum power ($P_{\rm STOT}$) observed at 1415 MHz with the Westerbork Synthesis Radio Telescope by Hummel (1980). As mentioned in the previous section, the central CO luminosities are in many cases lower limits to the total (or global) CO luminosities. In order to study statistically the dependence of CO luminosities on $L_{\rm IR}$, $L_{\rm B}$ and $P_{\rm STOT}$ we have estimated global CO luminosities in the following manner and also plotted them in Fig. 2.

We assume the distribution of CO to be Gaussian with an amplitude of $I_{\rm o}$ K km s^{-1} and a full half-power width of W pc. A statistical relation between the optical diameter D pc and W along the major axis of the galaxy is obtained by a study of 40 galaxies for which Young et al. (1995) have fitted Gaussians to the CO observations they made along the major axes. The median (Md) value for this ratio is given by $\mathrm{Md}(X) = \mathrm{Md}(W/D)$ and is found to be 0.14.

The observed central intensity is given by

$$I_{\rm obs} = I_{\rm o} / \sqrt{\left[1 + \left(\frac{FW}{W}\right)^2\right]\left[1 + \left(\frac{FW}{\cos i \cdot W}\right)^2\right]} \qquad (4)$$

assuming a Gaussian telescope beam of full half-power beamwidth FW in pc at the source, i is the inclination of the galaxy obtained from values in RC3. Therefore,

$$I_{\rm o} = I_{\rm obs} \cdot \sqrt{\left[1 + \left(\frac{FW}{W}\right)^2\right]\left[1 + \left(\frac{FW}{\cos i \cdot W}\right)^2\right]} \qquad (5)$$

and thus the global CO luminosity is given by

$$L_{\rm COg} = \frac{\pi}{4 \ln 2} I_{\rm obs} \cdot \sqrt{\{[D \cdot \mathrm{Md}(X)]^2 + FW^2\}\{\cos^2 i[D \cdot \mathrm{Md}(X)]^2 + FW^2\}} \qquad (6)$$

The blue luminosity of a galaxy is usually a measure of the star formation rate averaged over the past 3 10^9 years, and the infrared luminosity representative of the present star formation rate. The radio continuum is indicative of massive star formation as well as nuclear activity. The central CO luminosities of our sample of galaxies show a tight correlation with the IR luminosities, similar to that found by other investigators, wheras the central CO luminosities are somewhat more loosely correlated with the Blue luminosities. This difference in degree of correlation is to be expected since all blue galaxies may not necessarily be enriched in gas and dust but may have used up a larger amount of the interstellar matter in earlier epochs of rapid star formation. Alternatively, in the case of advanced mergers, the interstellar matter may have been collisionally removed from the parent galaxies.

Using global CO luminosities instead, as can be seen in Fig. 2, the correlations with both the IR luminosities and the radio continuum became looser but tightened somewhat with the Blue luminosities.

3.3. *CO maps of individual galaxies*

Figure 3 presents maps or partial maps of the CO profiles in thirteen of the galaxies observed with the 20-m OSO telescope. Each map contains an image of the galaxy obtained from the *Digitized Sky Survey*. The observed positions have been indicated with circles representing the half-power beamwidth of the 20-m telescope. The grids are centered on the positions given in Table 1. They are oriented North-South/East-West for the galaxies NGC 278, NGC 2782, NGC 3631, NGC 4194, NGC 5371 and NGC 6217. For the remaining galaxies, the orientations of the grids are along the major/minor axes as obtained from the Uppsala General Catalogue of Galaxies (Nilson 1973). The grid point spacing is either 15″ or 30″. (The galaxy UGC 2855 is also known by its alternative name A 0343.) We now briefly discuss some of these galaxies.

NGC 278 has a flocculent appearance with obvious large H II regions. It has an emission line spectrum that indicates active star formation processes (Schmidt et al. 1990). It has also a continuum radio source (Condon 1987). The CO is distributed in an unsymmetric fashion with some concentration towards the southeastern region.

NGC 772 is a large SA galaxy with asymmetric arm structure. It has faint H II regions (Oey & Kennicutt 1993) and a large H I radius (about 75 kpc) (Rao & Briggs 1993). There is a faint material bridge towards two dwarf companions and its satellite (NGC 770) has a retrograde orbit (Zaritsky et al. 1993). There is a tendency for CO emission to be present in all our observed positions; we have, however, only observed the inner region of the galaxy.

NGC 1055 has a prominent bulge; the spiral arm structure appears to be elevated above the galaxy's plane and obscures the upper half of the bulge (Shaw 1987). It is a binary galaxy together with NGC 1068 (Morgan & Hartwich 1988) and comprises a larger system with NGC 936, NGC 1084 and NGC 1087. Practically no CO is detected along the minor axis, but a clear velocity gradient is seen in the strong emission along the major axis.

UGC 2855 (or A 0343) is a fairly inconspicuous Sc galaxy which drew attention during the IRAS mission as a strong far-infrared source. It forms a pair together with UGC 2866 and both galaxies have been detected in the radio continuum at 4.85 GHz by Condon et al. (1991). UGC 2855 exhibits significant CO emission throughout the disk to large radii. Only the two outermost observed positions along the minor axis do not show any emission. These positions are, however, outside the optical part of the disk.

NGC 2276 is a spiral galaxy with multiple arm structure. We have mapped a substantial part of the galaxy with 15″ spacing. The CO is distributed in a lopsided fashion with more emission towards the northwestern region. We have also observed four positions 1′ from the centre along both major and minor axes but fail to detect any emission.

NGC 2782 is an "arm class 1" galaxy (Elmegreen & Elmegreen 1982b) which implies chaotic appearance, no symmetry and fragmented arms with different pitch angles. There is prominent diffuse optical component. The galaxy is an X-ray emitter (Fabbiano et al. 1992). CO is detected with certainty only in the central position. We failed to detect any emission outside 15″ from the centre.

NGC 3631 is fairly symmetrical with two major arms and several divisions. It forms a nearby group together with NGC 3178, NGC 3898, NGC 3953 and NGC 3992 in Ursa Major. It has had multiple supernova events (Richter & Rosa 1988). The galaxy is practically face-on. CO seems to be fairly evenly distributed with a smooth fall-off except in the southern direction where no emission is detected. No CO is detected beyond 30″ from the centre in any of the observed directions.

NGC 4194, the "Medusa" is a classical merger (Keel 1993). It has been observed in the Brγ infrared recombination line (De Poy 1993). It is found to be an example of an extreme star burst galaxy with 90% of the IR luminosity attributed to the star burst component (Prestwich et al. 1994). The CO luminosity is not particularly high. CO emission is observed out to 15″ from the centre.

NGC 4568 is a Sbc spiral which is in actual physical contact with its neighbour NGC 4567, they are members of the Virgo cluster. Fabbiano et al. (1992) have observed extended X-ray emission covering both galaxies and NGC 4568 has a recent type Ib/c supernova (van Dyk 1992). Extended radio emission has been observed by Condon (1987) at 1.49 GHz. Our CO data show strong CO emission along the major axis and also along the minor axis away from the companion. However, no CO is detected along the minor axis near the companion.

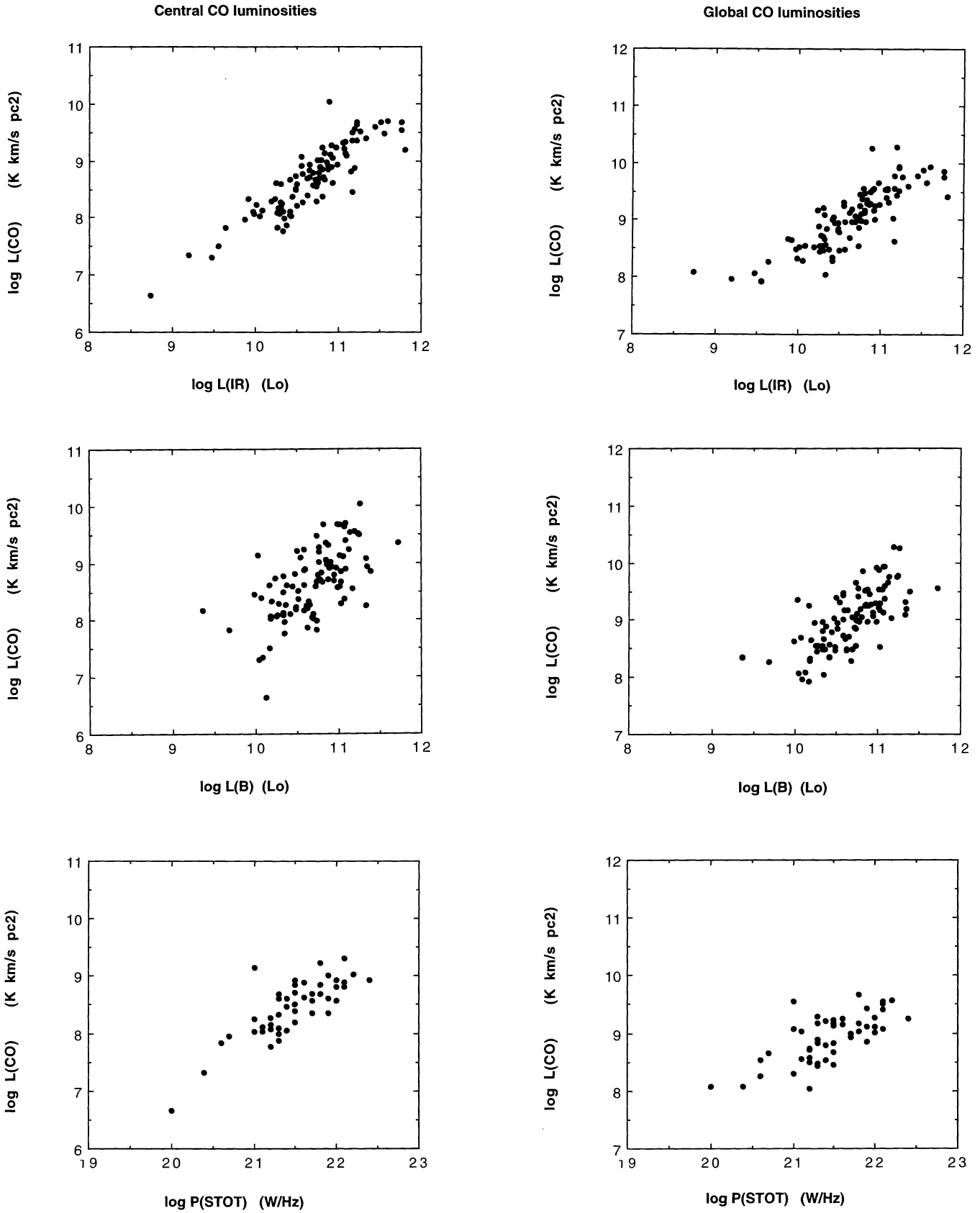

Fig. 2. Observed central and estimated global CO luminosities for the survey galaxies as functions of infrared (IR) and blue (B) luminosities and total radio power (P) at 1415 MHz

NGC 5218 is a classical interacting galaxy, its companion to the north is NGC 5216. The galaxies are gravitationally distorted and connected by an intergalactic bridge. CO is detected as far as 30″ northward along the minor axis towards the companion, but there is only sparse CO emission along the western major axis.

NGC 5371 is a grand design spiral galaxy (Elmegreen & Elmegreen 1990) with a rising H I rotation curve in the outer regions (Begeman 1987). It has also been classified as a LINER by Rush et al. (1993). It has a low dust temperature but substantial far-infrared luminosity and may be a good candidate for a post-starburst galaxy (Koorneef 1993). It is interesting that the strongest observed CO profile is at the 30″-position to the north along the major axis. Significant CO emission is also observed at the 15″-positions along the east-west bar.

NGC 6217 is characterized as a starburst galaxy by Calzetti et al. (1994). Observations of spectra dominated by stellar photoionization by Kennicutt (1992) and of extended radio emission at 1.4 and 5 GHz by Hummel et al. (1984) with the VLA support this classification. The CO emission is strongly peaked towards the centre of the galaxy.

NGC 7469 is a Seyfert 1 galaxy with extended IR emission (Surace et al. 1993), forming a pair with IC 5283. It has significant radio and X-ray emission and shows signs of violent star formation (Ulvestad et al. 1981; Condon et al. 1991; Fabbiano et al. 1992). It has a strong central CO emission source which is extended along the major axis.

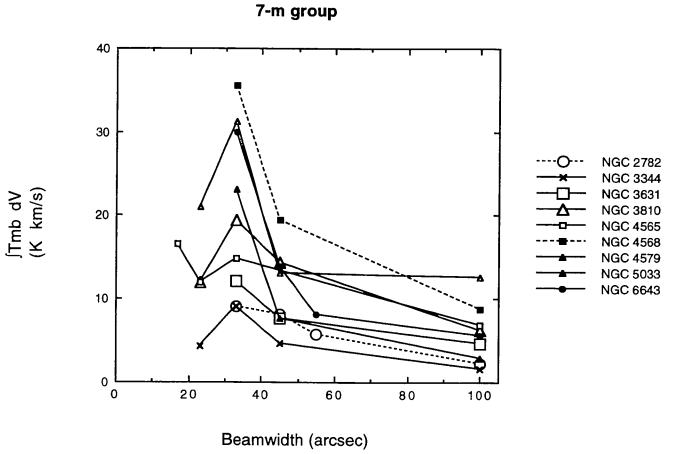

Fig. 4. The variation of the $J = 1-0$ CO integrated intensity, $I_{CO} = \int T_{mb}\ dV$ (K km s^{-1}), for a sample of nine galaxies (which have been also been observed with specifically the Bell Labs 7-m telescope) as a function of the FWHM beamwidth (arcsec) of the mm-wave telescope used for the observations. The solid curves represent a velocity range of 600–1500 km s^{-1}, the dashed curves 2200–2550 km s^{-1}

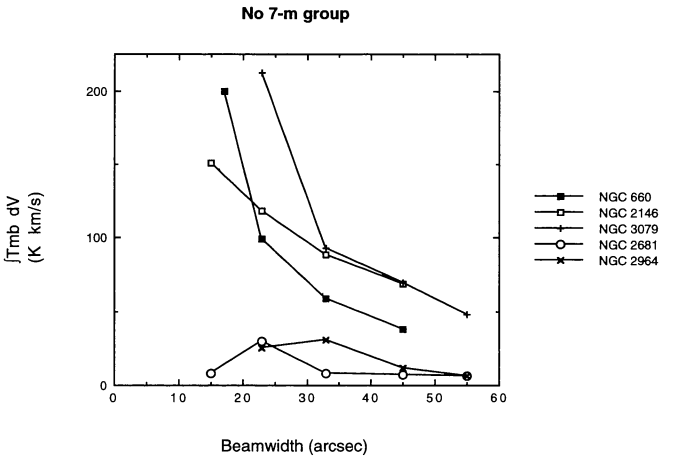

Fig. 5. The variation of the $J = 1-0$ CO integrated intensity, $I_{CO} = \int T_{mb}\ dV$ (K km s^{-1}), for a sample of five galaxies as a function of the FWHM beamwidth (arcsec) of the mm-wave telescope used for the observations

4. Comparison with previous observations

A number of galaxies have by now been observed using telescopes with quite a range of diameters (see Col. 11 in Table 1) and it is therefore of certain interest to compare the different observations. We are well aware of calibration uncertainties of the order of at least 10% (Mirabel et al. 1990) when comparing data taken with different telescopes. In some cases these uncertainties may be considerably higher. Nevertheless there are clear tendencies which we now describe.

In Figs. 4 and 5, we present the results of a comparison of observations of some of these galaxies, which have been observed with telescopes having different beamwidths ranging from 100″ to 15″ - Bell Labs 7-m, NRAO 12-m, FCRAO 14-m, OSO 20-m (this paper), IRAM 30-m and NRO 45-m. We have plotted the CO integrated intensity, $I_{CO} = \int T_{mb}\ dV$, as a function of the half-power beamwidth for some galaxies which are relatively close by and which have large optical diameters. In Fig. 4 we have included all the galaxies in our sample which have been observed with the Bell Labs 7-m telescope and thus the largest beamwidth, namely 100″. Most of these galaxies have radial velocities in the range 600–1500 km s^{-1}, but two (indicated with dashed lines) have radial velocities in the range 2200–2550 km s^{-1}. In Fig. 5 we have plotted the results for three galaxies with very high integrated intensities, namely NGC 660, NGC 2146 and NGC 3079 (radial velocity range of 880–1150 km s^{-1}), and for two other galaxies, NGC 2681 and NGC 2964 (radial velocity range of 680–1325 km s^{-1}).

Two definite tendencies can be discerned in Figs. 4 and 5 which we interpret as reflecting different distributions of the CO throughout the galaxies. One shows a fast dropoff of integrated intensity with increasing beamwidth, in

the other case the integrated intensity remains relatively constant with increasing beamwidth. In the former case (e.g. NGC 660, NGC 2146 and NGC 3079), the CO has a component which is strongly concentrated to the centre of the galaxy - there is some indication of a core depletion in the central CO concentration in a few other galaxies (e.g. NGC 2681, NGC 3810 and NGC 5033). In some cases (e.g. NGC 2782 and NGC 4565) there is very little variation in the integrated intensity with beamwidth, which implies a uniform distribution throughout the observed part of the galaxy.

5. Conclusion

A $J = 1-0$ CO line survey of 168 galaxies has been performed using the 15-m SEST and the 20-m OSO millimetre wave telescope during 1985-1988. CO has been detected in 101 galaxies, about a fifth of these are new detections. Comparison with previous observations indicate variations which can be attributed to differences in the distribution of the CO in the galaxies being sampled with various resolutions. There is also clear evidence in our sample for barred galaxies to be more likely CO-rich than non-barred galaxies. Thirteen galaxies have been (partially) mapped using the 20-m OSO telescope.

Acknowledgements. We should like to thank Helmuth Kristen and Per A.B. Lindblad for help in preparing the images of the galaxies presented in Fig. 3. The Swedish-ESO Submillimetre Telescope, SEST, is operated jointly by ESO and the Swedish National Facility for Radio Astronomy, Onsala Space Observatory at Chalmers University of Technology. This research has made use of the SIMBAD database, operated at CDS, Strasbourg, France.

References

Aalto S., Black J.H., Johansson L.E.B., Booth R.S., 1991, A&A 249, 323
Afanas'ev V.L., Zasov A.V., Popravko G.V., Sil'chenko O.K., 1991, SvAL 17, 325
Baan W.A., Rhoads J., Haschick A.D., 1992, ApJ 401, 508
Balzano V.A., 1983, ApJ 268, 602
Beck R., 1991, Magnetic Fields in Spiral Galaxies. In: Duric N., Crane P.C. (eds.), The Interpretation of Modern Synthesis Observations of Spiral Galaxies. Astron. Soc. Pac. Conf. Ser. 18, 43
Beckman J.E., Cepa J., 1990, A&A 229, 37
Bergeman, 1987, PhD Thesis, Groningen University
Braine J., Combes F., 1992, A&A 264, 433
Braine J., Combes F., Casoli F., et al., 1993, A&AS 97, 887
Brandt W.N., Fabian A.C., Nandra K., Tsuruta S., 1993, MNRAS 265, 996
Calzetti D., Kinney A.L., Storchi-Bergmann T., 1994, ApJ 429, 582
Chini R., Krügel E., Lemke R., Ward-Thompson D., 1995, A&A 295, 317
Chini R., Krügel E., Steppe H., 1992, A&A 255, 87
Condon J.J., 1987, ApJS 65, 485
Condon J.J., Condon M.A., Gisler G., Puschell J.J., 1982, ApJ 252, 102
Condon J.J., Frayer D.T., Broderick J.J., 1991, AJ 101, 362
De Poy, 1993, ApJ
de Vaucouleurs G., de Vaucouleurs A., Corwin Jr. H.G., et al., 1991, "Third Reference Cataloque of Bright Galaxies". Springer, New York, (RC3)
Devereux N., Taniguchi Y., Sanders D.B., Nakai N., Young J.S., 1994, AJ 107, 2006
Elmegreen D.M., Elmegreen B.G., 1982a, AJ 87, 626
Elmegreen D.M., Elmegreen B.G., 1982b, MNRAS 201, 1021
Elmegreen D.M., Elmegreen B.G., 1990, ApJ 364, 412
Fabbiano G., Kim D.-W., Trinchieri G., 1992, ApJS 80, 531
Filippenko A.V., Sargent W.L.W., 1992, AJ 103, 28
Freudling W., Martel H., Haynes M.P., 1991, ApJ 377, 349
Gallimore J.F., Baum S.A., O'Dea C.P., Brinks E., Pedlar A., 1994, ApJ 422, L13
Guhathakurta P., van Gorkom J.H., Kotanyi C.G., Balkowski C., 1988, AJ 96, 851
Heckman T.M., Blitz L., Wilson A.S., Armus L., Miley G.K., 1989, ApJ 342, 735
Huchtmeier W.K., Richter O.-G., 1989, "A General Catalog of HI Observations of Galaxies". Springer, New York
Hummel E., 1980, A&AS 41, 151
Hummel E., Jörsäter S., Lindblad P.O., Sandqvist Aa., 1987, A&A 172, 51
Hummel E., van der Hulst J.M., Dickey J.M., 1984, A&A 134, 207
Jackson J.M., Snell R.L., Ho P.T.P., Barrett A.H., 1989, ApJ 337, 680
Jörsäter S., van Moorsel G., 1995, AJ 110, 2037
Kawara K., Nishida M., Gregory B., 1987, ApJ 321, L35
Keel W.C., 1983, ApJS 52, 229
Keel W.C., 1987, A&A 172, 43
Keel W.C., 1993, Mercury 22, 44
Kenney J.D.P., Wilson C.D., Scoville N.Z., Devereux N.A., Young J.S., 1992, ApJ 395, L79
Kennicutt R.C., 1992, ApJ 388, 310
Koorneef J., 1993, ApJ 403, 581
Kyazumov G.A., 1980, SvAL 6, 220
Lutz D., 1992, A&A 259, 462
Mirabel I.F., Booth R.S., Garay G., Johansson L.E.B., Sanders D.B., 1990, A&A 236, 327
Morgan C.G., Hartwick F.D.A., 1988, ApJ 328, 381
Neff S.G., Hutchings J.B., Stanford S.A., Unger S.W., 1990, AJ 99, 1088
Nilson P., 1973, "Uppsala General Catalogue of Galaxies", Uppsala Observatory (UGC)
Olofsson H., 1983, Ph. D. thesis, Chalmer University Technical Report No. 139
Osman A.M.I., 1986, Ap&SS 124, 345
Oye M.S., Kennicutt Jr. R.C., 1993, ApJ 411, 137
Prestwick A.H., Joseph R.D., Wright G.S., 1994, ApJ 422, 73
Rao S., Briggs F., 1993, ApJ 419, 515
Richmond M.W., Knapp G.R., 1986, AJ 91, 517
Richter O.-G., Rosa M., 1988, A&A 206, 219
Rickard L.J., Palmer P., Morris M., Zuckerman B., Turner B.E., 1975, ApJ 199, L75
Roche P.F., Chandler C.J., 1993, MNRAS 265, 486
Rots A.H., 1980, A&AS 41, 189

Rubin V.C., Ford Jr. W.K., Thonnard N., 1978, ApJ 225, L107
Rubin V.C., Kenney J.D., Boss A.P., Ford Jr. W.K., 1989, AJ 98, 1246
Rush B., Malkan M.A., Spinoglio L., 1993, ApJS 89, 1
Sage L.J., 1993, A&A 272, 123
Sage L.J., 1993, A&AS 100, 537
Saikia D.J., Pedlar A., Unger S.W., Axon D.J., 1994, MNRAS 270, 46
Sanders D.B., Mirabel I.F., 1985, ApJ 298, L31
Sanders D.B., Scoville N.Z., Soifer B.T., 1991, ApJ 370, 158
Sanders D.B., Scoville N.Z., Young J.S., et al., 1986, ApJ 305, L45
Sandqvist Aa., Elfhag T., Jörsäter S., 1988, A&A 201, 223
Sandqvist Aa., Jörsäter S., Lindblad P.O., 1982, A&A 110, 336
Sandqvist Aa., Jörsäter S., Lindblad P.O., 1995, A&A 295, 585
Schmidt A.A., Bica E., Alloin D., 1990, MNRAS 243, 620
Schwartz R.D., 1978, PASP 90, 393
Schöniger F., Sofue Y., 1994, A&A 283, 21
Scoville N.Z., Sanders D.B., Sargent A.I., Soifer B.T., Tinney C.G., 1989, ApJ 345, L25
Shaw M.A., 1987, MNRAS 229, 691
Sofue Y., 1994, PASJ 46, 173
Sofue Y., Irwin J.A., 1992, PASJ 44, 353
Sofue Y., Nakai N., 1994, PASJ 46, 147
Solomon P.M., Downes D., Radford S.J.E., 1992, ApJ 387, L55
Solomon P.M., Sage L.J., 1988, ApJ 334, 613
Stanford S.A., Bushouse H.A., 1991, ApJ 371, 92
Stark A.A., Elmegreen B.G., Chance D., 1987, ApJ 322, 64
Stark A.A., Knapp G.R., Bally J., Wilson R.W., Penzias A.A., Rowe H., 1986, ApJ 310, 660
Stauffer J.R., 1982, ApJS 50, 517
Surace J.A., Mazzarella J., Soifer B.T., Wehrle A.E., 1993, AJ 105, 864
Tacconi L.J., Tacconi-Garman L.E., Thornley M., van Woerden H., 1991, A&A 252, 541
Taniguchi Y., Kameya O., Nakai N., Kawara K., 1990, ApJ 358, 132
Taniguchi Y., Murayama T., Nakai N., Suzuki M., Kameya O., 1994, AJ 108, 468
Tifft W.G., Cocke W.J., 1988, ApJS 67, 1
Tinney C.G., Scoville N.Z., Sanders D.B., Soifer B.T., 1990, ApJ 362, 473
Ulvestad J.S., Wilson A.S., Sramek R.A., 1981, ApJ 247, 419
van der Hulst J.M., Crane P.C., Keel W.C., 1981, AJ 86, 1175
van Driel W., Combes F., Casoli. M., Gerin M., Nakai N., et al., 1995, AJ 109, 942
van Dyk S.D., 1992, AJ 103, 1788
Verter F., 1990, PASP 102, 1281
Wiklind T., Henkel C., 1989, A&A 225, 1
Wiklind T., Henkel C., Sage L.J., 1993, A&A 271, 71
Wilson A.S., Helfer T.T., Haniff C.A., Ward M.J., 1991, ApJ 381, 79
Wilson R.W., Jefferts K.B., Penzias A.A., 1970, ApJ 161, L43
Xie S., Young J., Schloerb F.P., 1994, ApJ 421, 434
Young J.S., Schloerb F.P., Kenney J.D., Lord S.D., 1986, ApJ 304, 443
Young J.S., Xie S., Tacconi L., et al., 1995, ApJS 98, 219
Young J.S., Xie S., Kenney J.D.P., Rice W.L., 1989, ApJS 70, 699
Zaritsky D., Smith R., Frenk C., White S.D.M., 1993, ApJ 405, 464

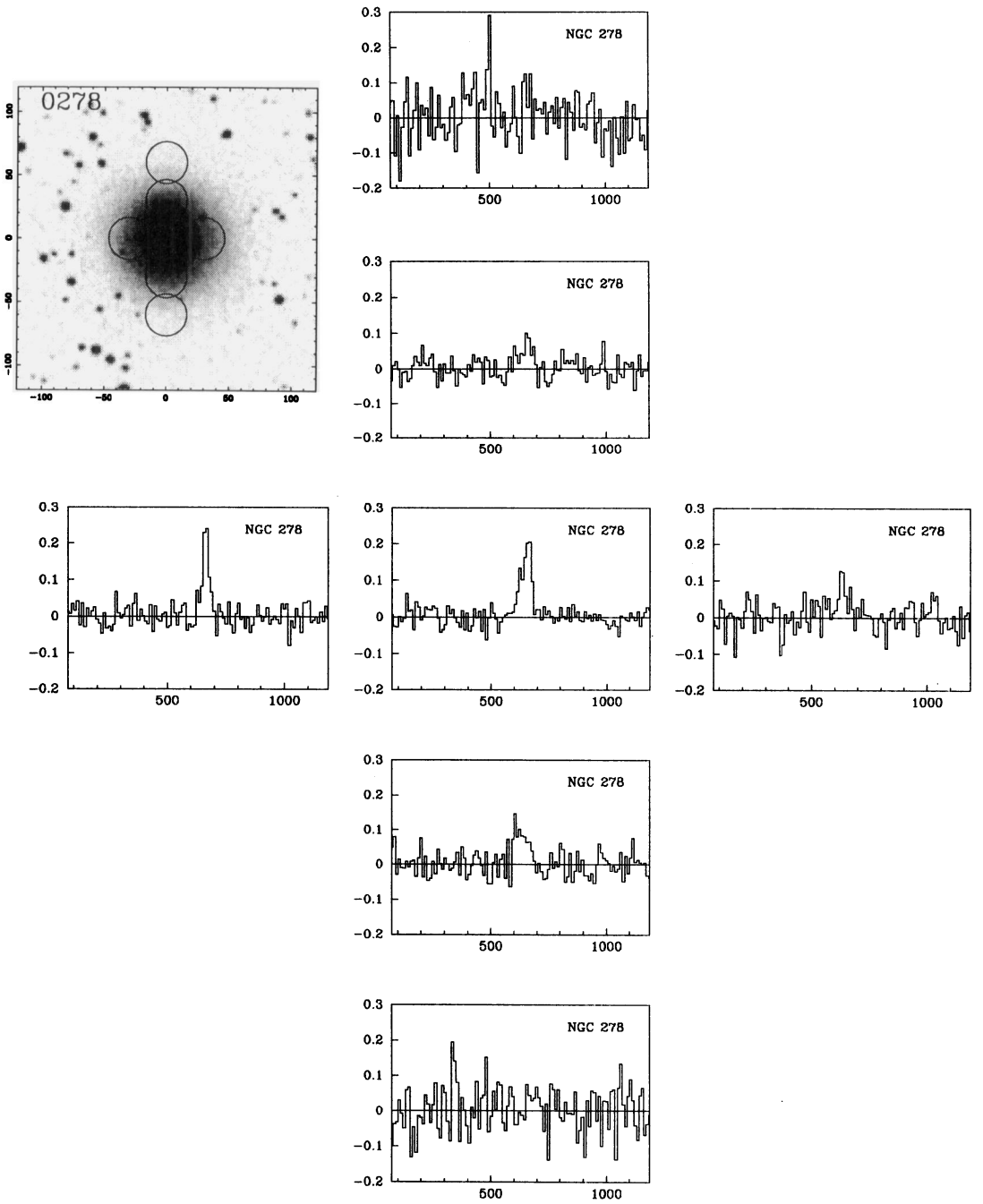

Fig. 3. $J = 1-0$ CO profile maps of 13 galaxies. The observing grids, with grid spacings of 15″ or 30″, are centered on the positions listed in Table 1 and oriented equatorially (epoch 1950.0) or along the major/minor axes. The optical images are from the Digitized Sky Survey and the circles represent the positions of the 33″-beam of the 20-m OSO telescope

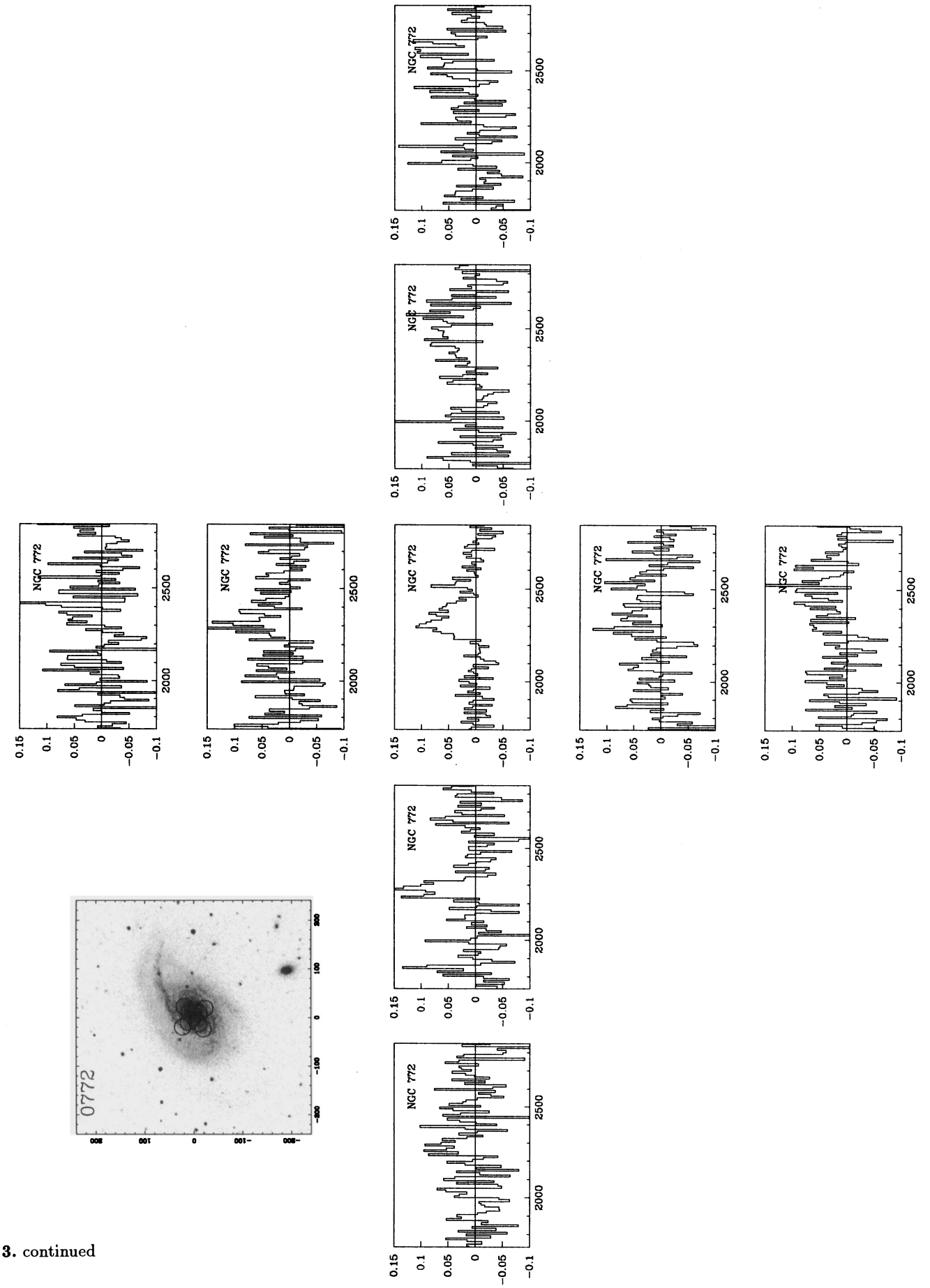

Fig. 3. continued

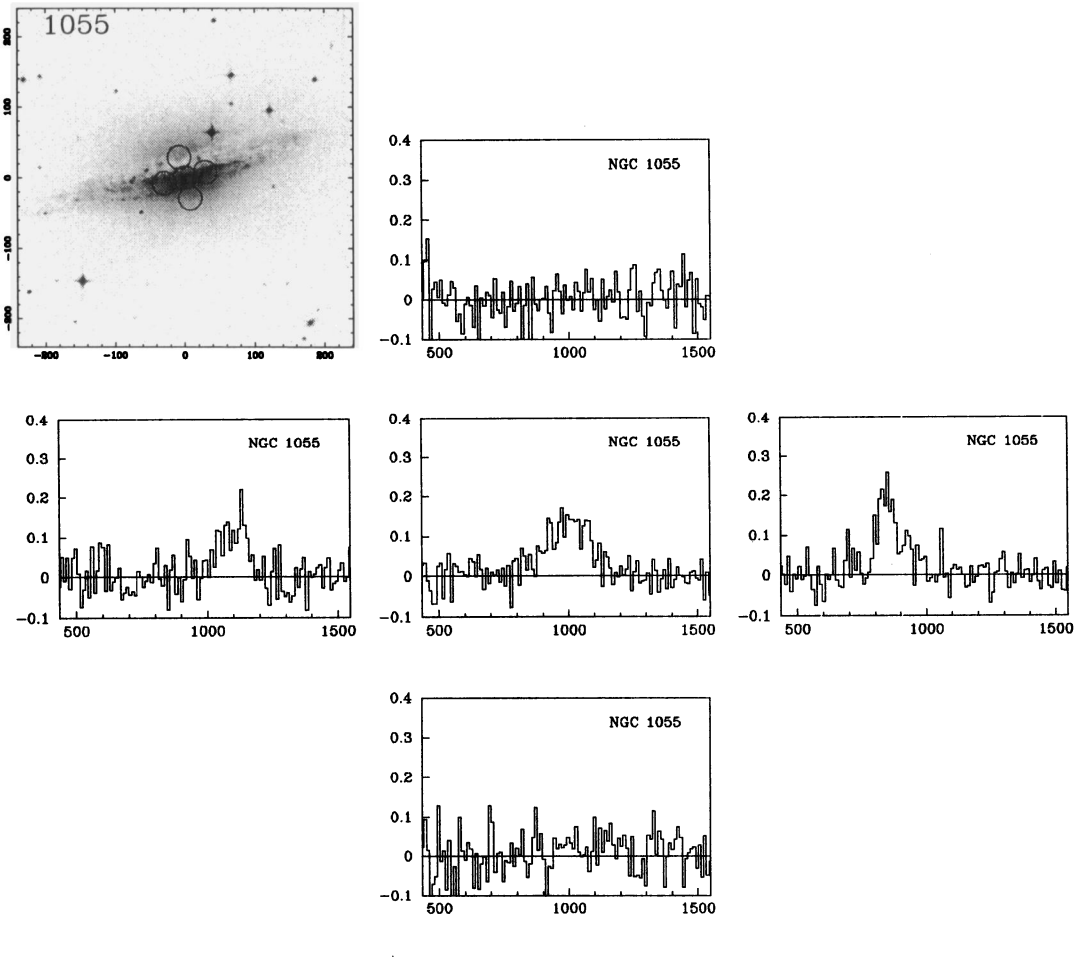

Fig. 3. continued

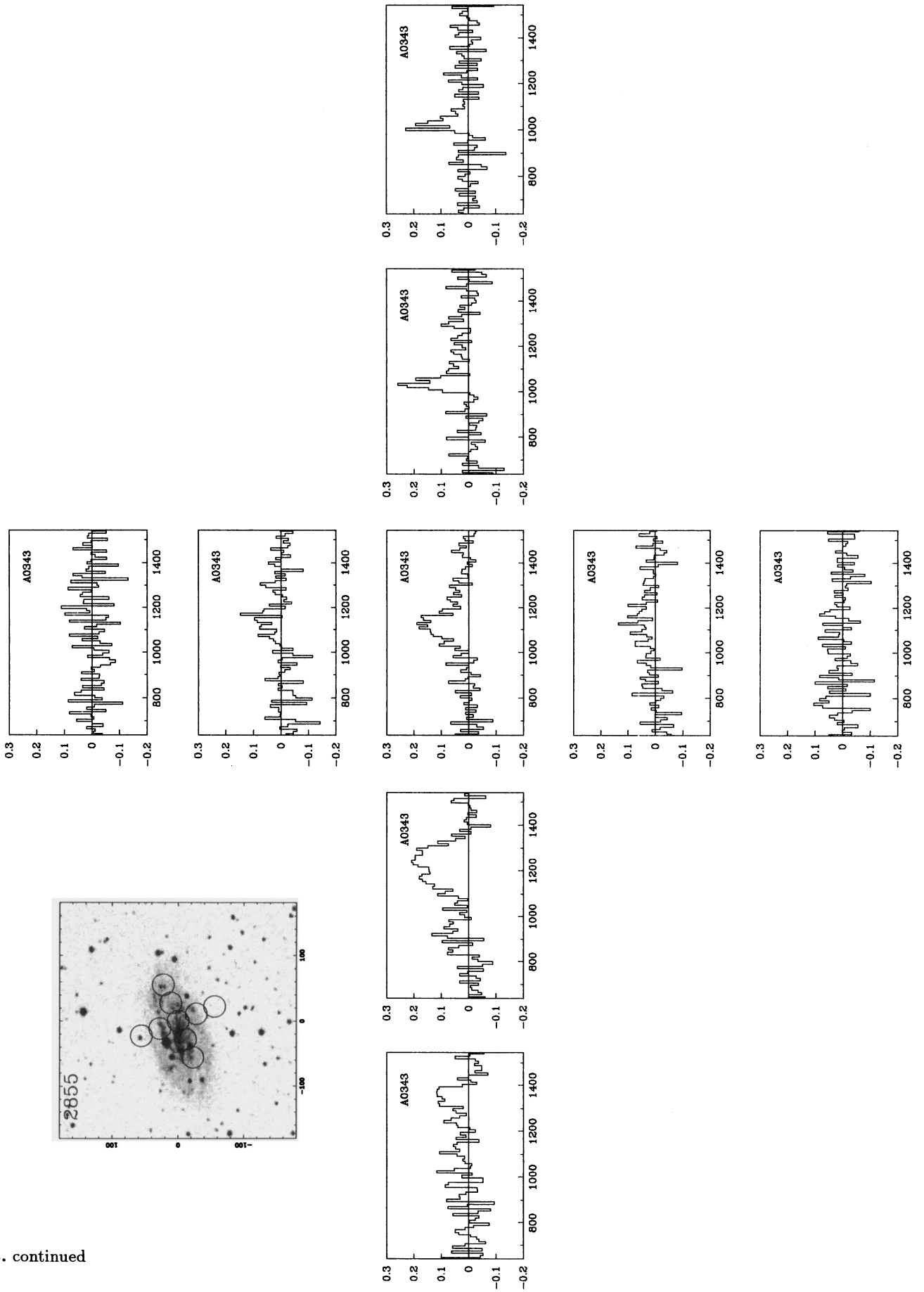

Fig. 3. continued

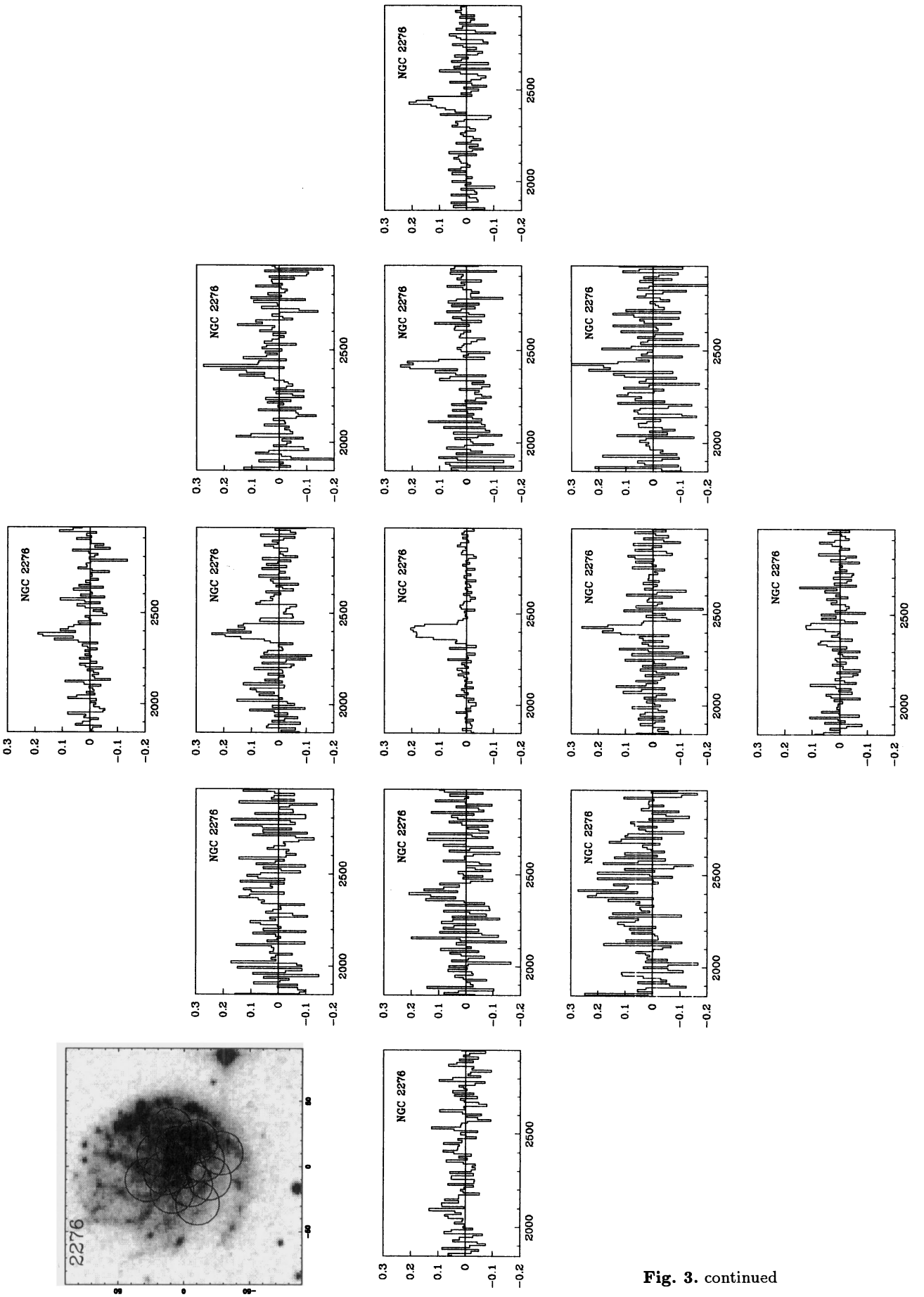

Fig. 3. continued

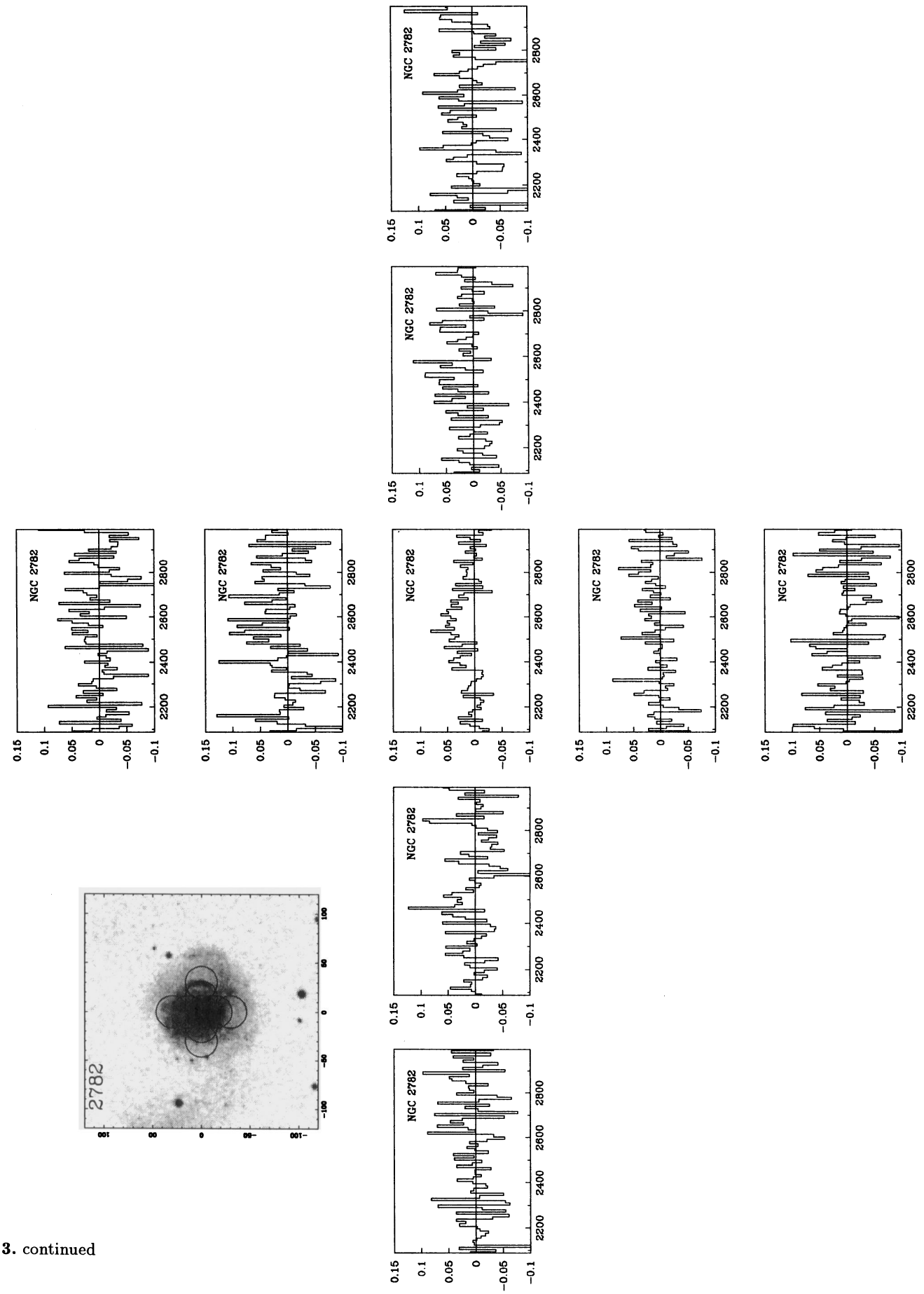

Fig. 3. continued

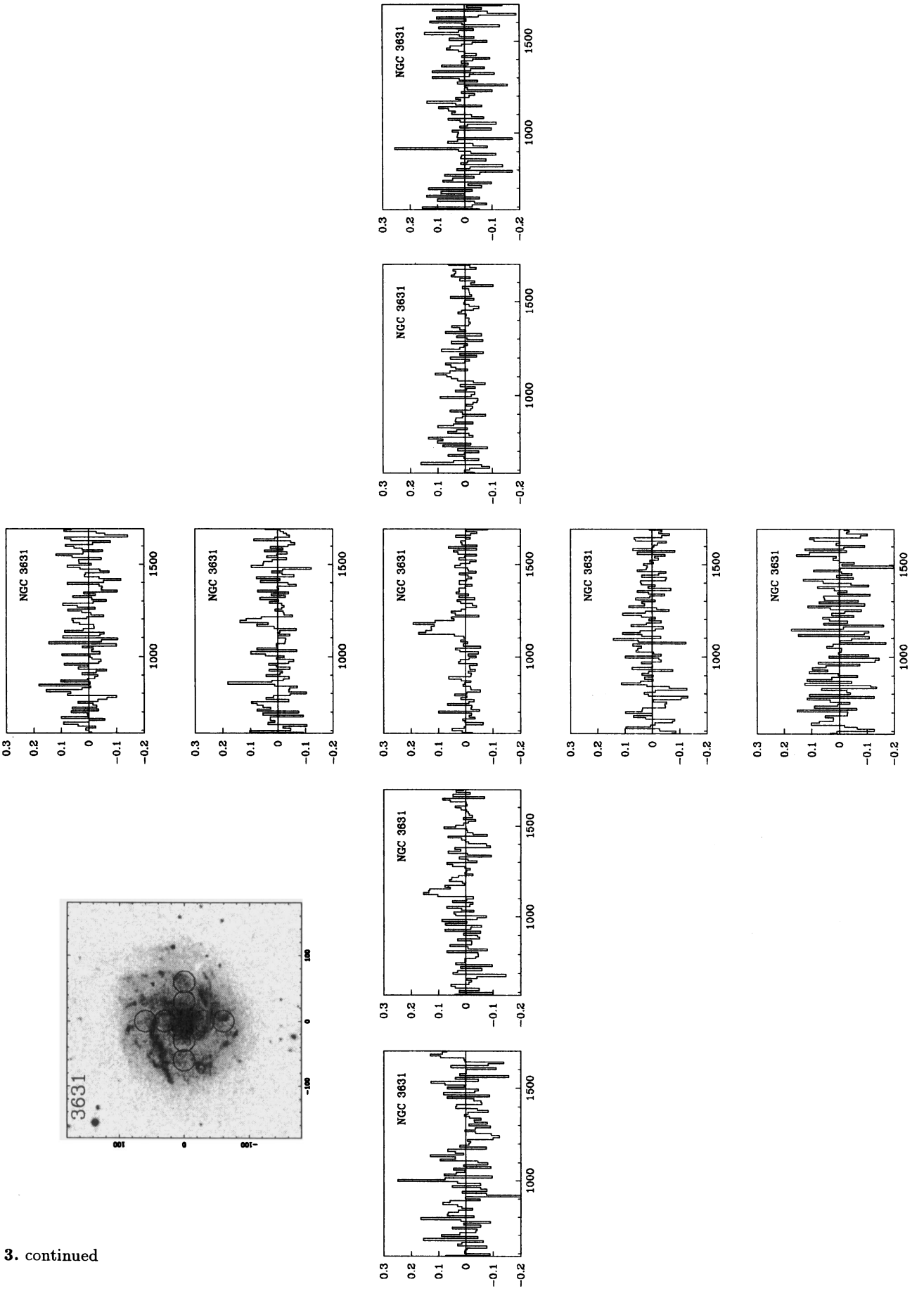

Fig. 3. continued

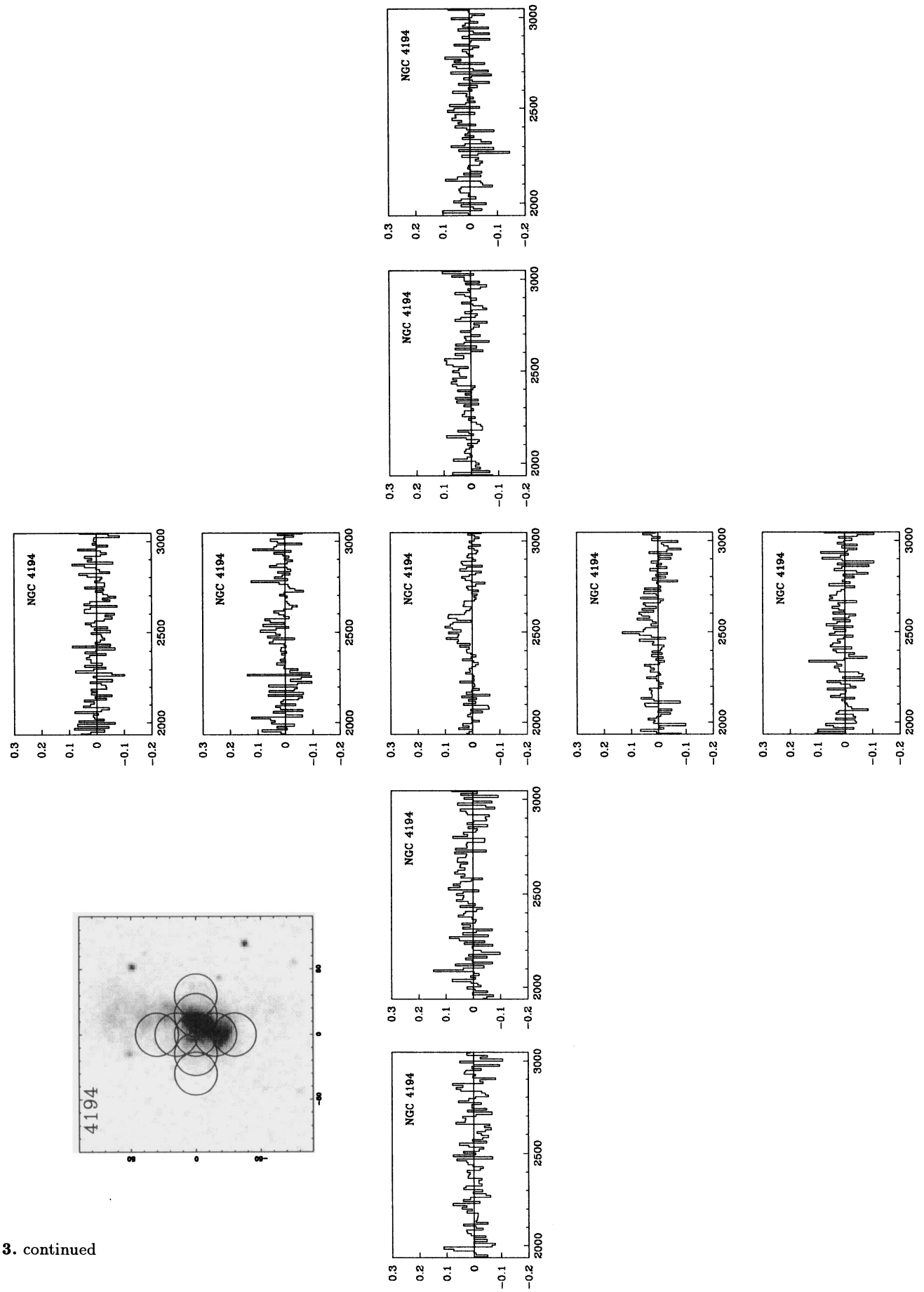

Fig. 3. continued

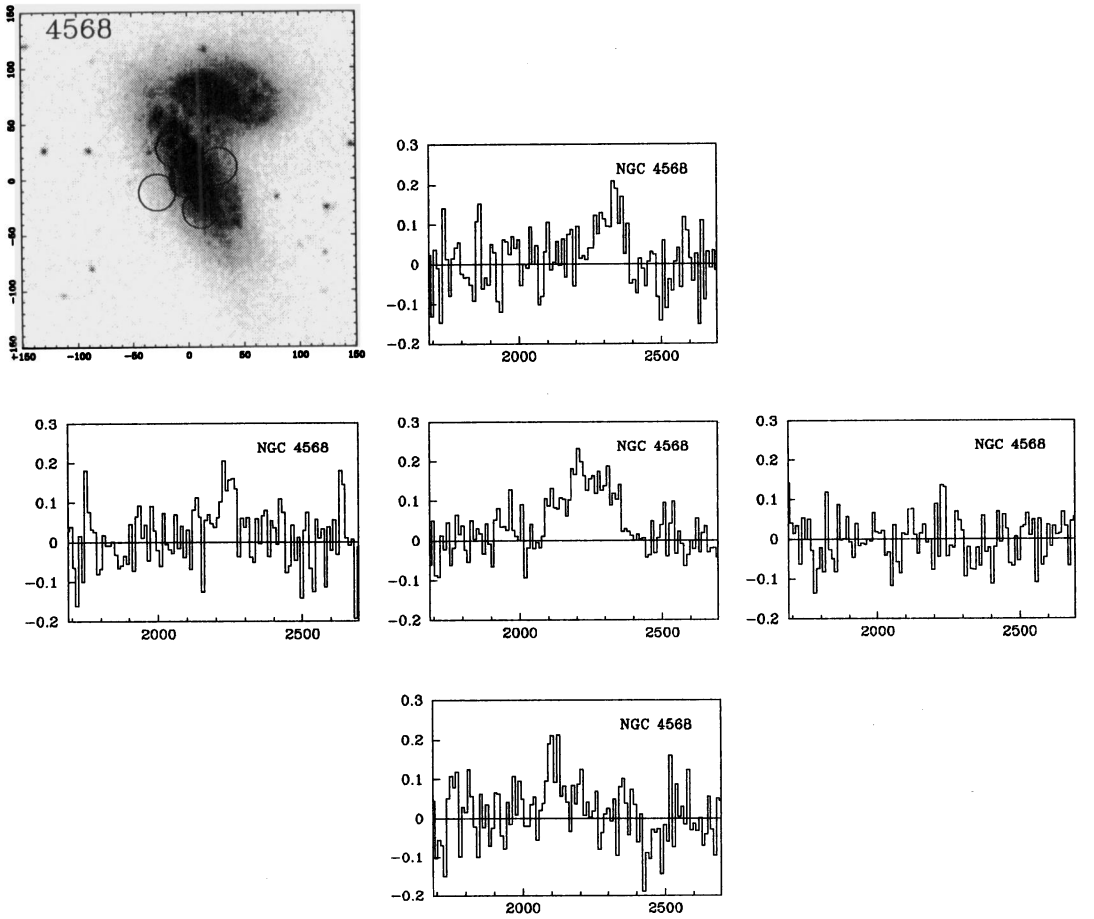

Fig. 3. continued

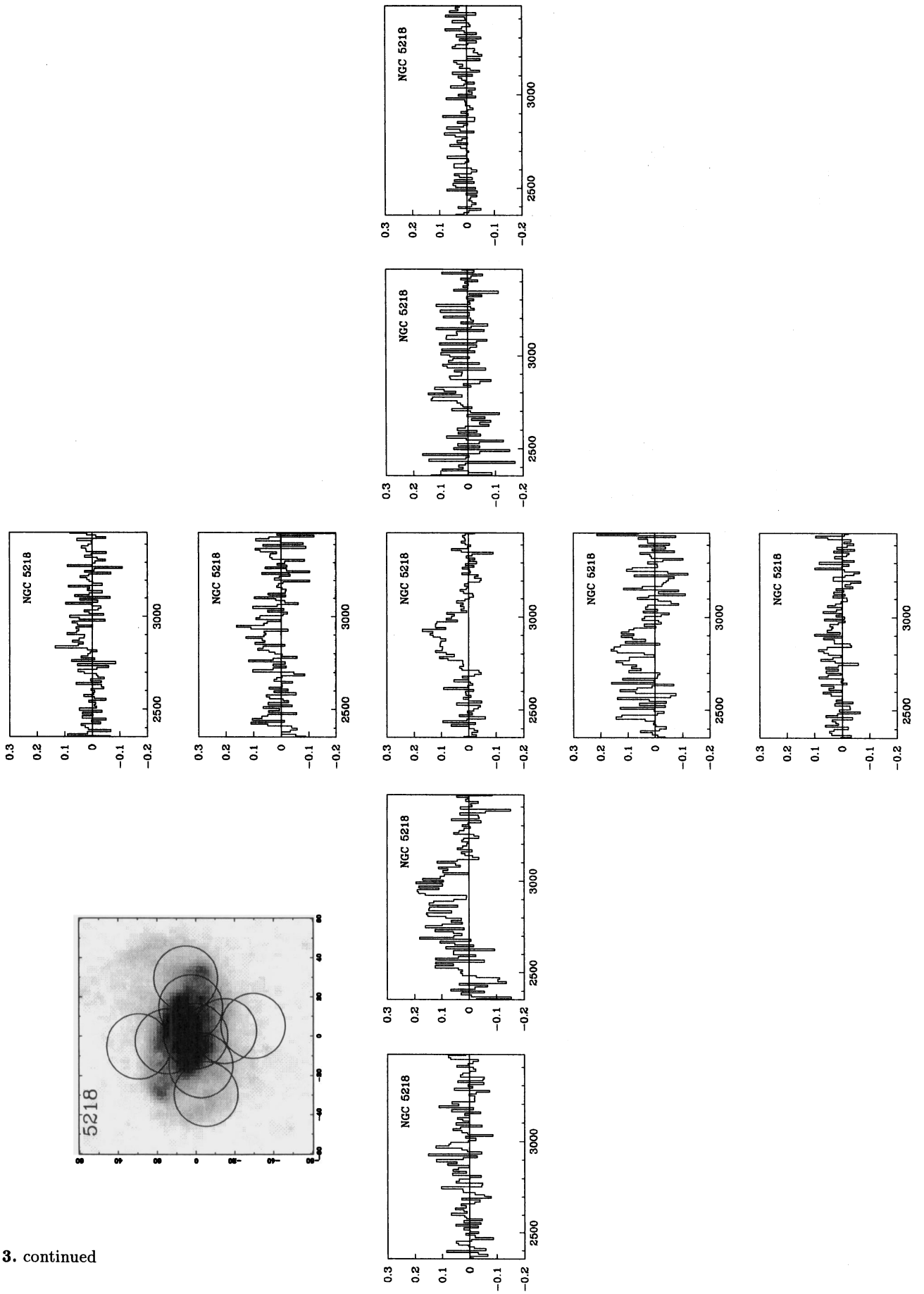

Fig. 3. continued

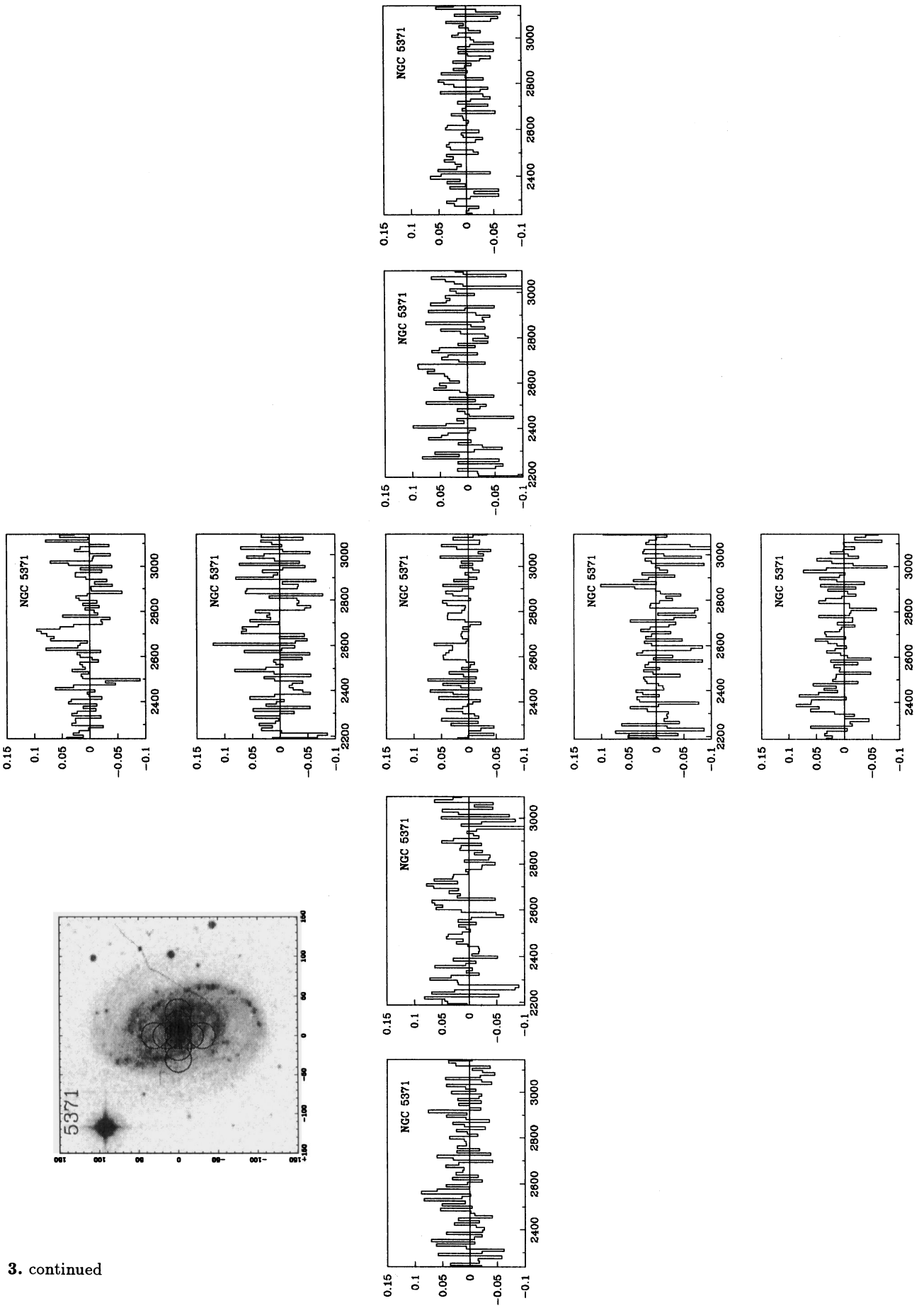

Fig. 3. continued

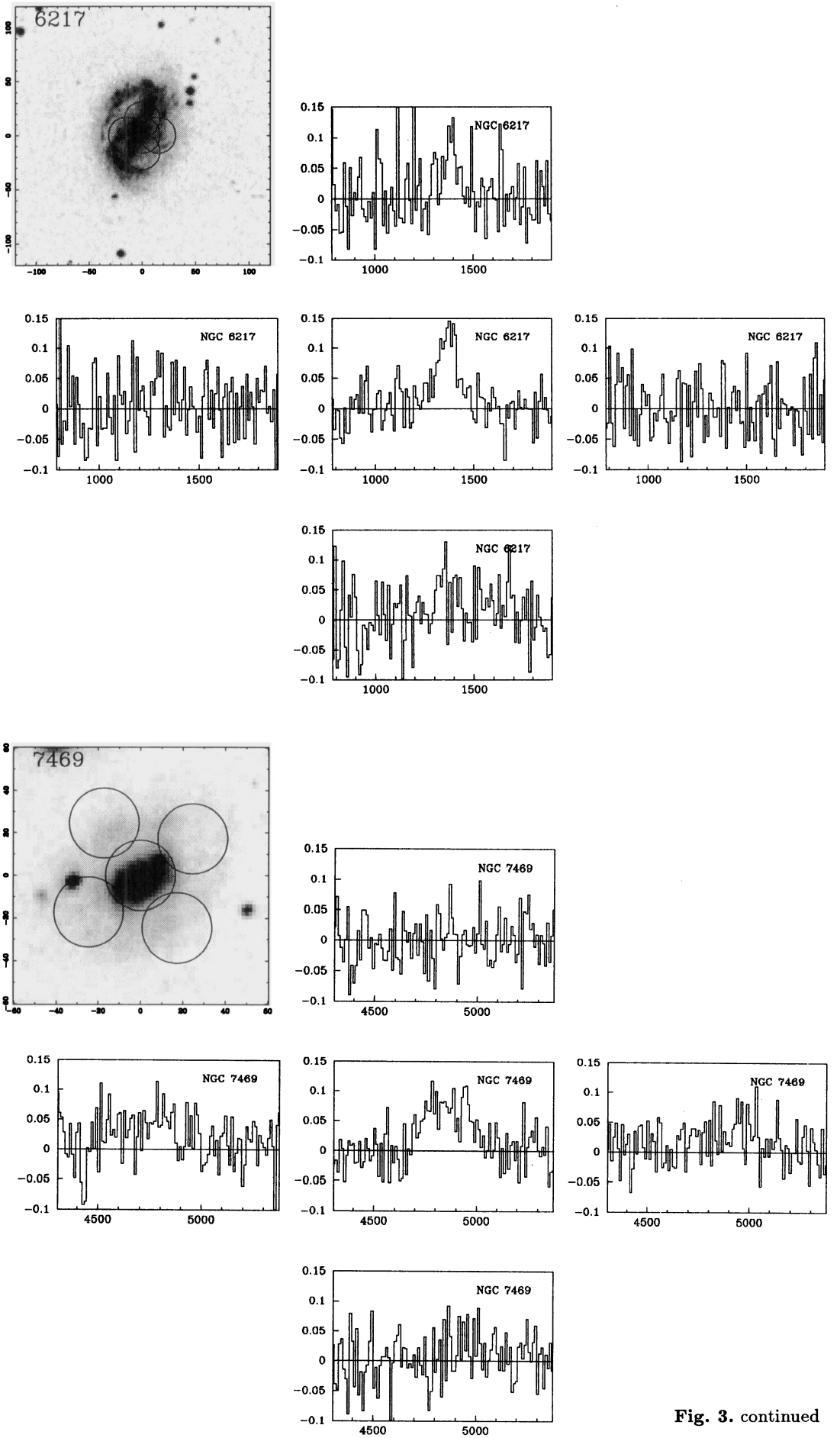

Fig. 3. continued